NON-LINEAR FLUTTER

Thesis by

Edward Richard Fleming

In Partial Fulfillment of the Requirements

For the Degree of

Doctor of Philosophy

California Institute of Technology

Pasadena, California

1960

ACKNOWLEDGMENT

The author wishes to express his gratitude for assistance received from several sources during the conduct of this research; first to Doctor Y. C. Fung who suggested the project and made valuable comments during the investigation; to the Douglas Aircraft Company whose computing facilities were used for a portion of the numerical analysis and whose support made it possible for the author to attend graduate school and conduct the present work. Last, it is with special pleasure that the author thanks his thesis advisor, Doctor T. K. Caughey, whose assistance and encouragement throughout the project was much appreciated.

ABSTRACT

The problem of two degree of freedom flutter in the presence of structural non-linearities is investigated. The specific problem chosen for investigation is that of bending-torsion flutter of a two-dimensional airfoil in a supersonic flow. The Kryloff-Bogoliuboff assumption of nearly sinusoidal response with slowly varying amplitude and phase is made and aerodynamic piston theory is used throughout the analysis.

Formulas for flutter limit cycles are developed in terms of general structural non-linearities. Necessary and sufficient conditions are developed for the existence of stable flutter limit cycles in the case of an airfoil with non-linear torsional stiffness. Several numerical examples of this case are given including a case which exhibits flutter for large disturbances but is stable at all airspeeds for small disturbances.

An analog computer investigation of flutter dependence on initial conditions is given.

TABLE OF CONTENTS

LIST OF SYMBOLS

a_∞ = speed of sound in the undisturbed flow (ft/sec)

b = airfoil semi-chord (ft)

C_α = torsion spring control function (lb)

C_h = bending spring control function (lb/ft)

$f_1(h)$ = deviation from linearity of the bending spring

$f_2(\alpha)$ = deviation from linearity of the torsion spring

h = bending deflection (ft)

h_o = amplitude of oscillatory bending deflection (ft)

I_α = pitching moment of inertia about the elastic axis (lb sec^2)

k = reduced frequency $\left(\frac{\omega b}{U}\right)$

M = Mach number

m = airfoil mass per unit span $\left(\frac{\text{lb sec}^2}{\text{ft}^2}\right)$

ρ^2 = squared dimensionless airfoil radius of gyration about the airfoil center of gravity

P = elastic axis parameter $(1 - 2x_o)$

Q = elastic axis parameter $\left(\frac{4}{3} - 4x_o + 4x_o^2\right)$

R = frequency ratio $\left(\frac{\omega_h}{\omega_\alpha}\right)^2$

r_α = dimensionless pitching radius of gyration about the elastic axis

U = airfoil forward speed (ft/sec)

x_o = dimensionless elastic axis location

x_α = dimensionless airfoil center of gravity location

X = frequency ratio

α = airfoil torsional displacement, angle of attack (radians)

Δ = frequency separation parameter

ϵ = small parameter identified with the deviation from linearity of the bending and torsion springs

η = perturbation parameter for stability study

λ = airspeed-mass ratio parameter $\left(\frac{1}{\mu M}\right)$

μ = mass ratio $\left(\frac{m}{4\rho_\infty b^2}\right)$

ξ = perturbation parameter for stability study

ρ_∞ = air density in the undisturbed flow (slugs/ft^3)

τ = dimensionless time $\left(\frac{Ut}{b}\right)$

φ = phase angle (radians)

ω_h = reference frequency for bending spring (rad/sec)

ω_α = reference frequency for torsional spring (rad/sec)

ω = frequency of oscillation (rad/sec)

In additions to the above symbols further notation was employed to facilitate presentation. The principal symbols used in this manner were:

$$A = K^2(\beta^2 - r_\alpha^2 R \Sigma)$$

$$B = \lambda K (P x_\alpha - r_\alpha^2)$$

$$C = K^2 \Sigma r_\alpha^2 x_\alpha + \lambda (P x_\alpha - r_\alpha^2)$$

$$D = \lambda K (Q x_\alpha - P r_\alpha^2)$$

$$E = K^2 \Sigma R x_\alpha$$

$$F = \lambda K (x_\alpha - P)$$

$$G = K^2(\beta^2 - r_\alpha^2 \Sigma) + \lambda (x_\alpha - P)$$

$$H = \lambda K (P x_\alpha - Q)$$

$$\mu(\alpha_0) = \frac{\epsilon K^2 \bar{X} r_\alpha^2}{\pi \alpha_0} \int_0^{2\pi} f_2(\alpha_0 \sin\theta_2) \sin\theta_2 \, d\theta_2$$

$$= \epsilon K^2 \bar{X} r_\alpha^2 \, g_2(\alpha_0)$$

$$\mu'(\alpha_0) = \frac{d\mu(\alpha_0)}{d\alpha_0}$$

$$\nu\left(\frac{h_0}{b}\right) = \frac{\epsilon k^2 \bar{X} R}{\pi \frac{h_0}{b}} \int_0^{2\pi} f_1\left(\frac{h_0}{b} \sin\theta_1\right) \sin\theta_1 \, d\theta_1$$

$$= \epsilon k^2 \bar{X} R \, g_1\left(\frac{h_0}{b}\right)$$

CHAPTER I

INTRODUCTION

The study of aeroelasticity consists of the application of the laws of classical mechanics to problems which arise in the flight of deformable vehicles through an atmosphere. Within the broad framework of classical mechanics the disciplines most pertinent to aeroelasticity are those of fluid mechanics and elasticity. Each of these, in its fundamental formulation, is mathematically non-linear and it is thus not surprising that non-linear problems occur in the study of aeroelasticity. In view of the extreme mathematical difficulty usually associated with the solution of non-linear problems it is fortunate for the aeroelastician that linearized formulations of the laws of elasticity and fluid mechanics usually yield sufficient accuracy for most of his problems. There are exceptions to this, however, and occasions arise in which non-linearity cannot be ignored. One such exception is the problem of stall flutter. Another is suggested by the aerodynamic heating associated with high flight speeds which introduces non-linear structural characteristics. Still another exceptional situation is encountered when unusual control systems introduce non-linearities which influence structural responses.

Even excluding the exceptional cases, however, the fundamental non-linearity of the foundations of aeroelasticity suggests that characteristics peculiar to non-linear systems will occur in all aeroelastic problems. It is well known that linear analyses fail to predict these factors and it was thus considered desirable to examine a particular aeroelastic problem in the light of non-linear theory. This is an admittedly academic point of view for most problems, but should have the effect of showing at least qualitatively the type of limiting behavior to be expected from certain aeroelastic systems. It should also be mentioned that, for dominantly non-linear problems of the type mentioned above, the non-linear point of view is essential to obtaining quantitative results.

The problem chosen for investigation in the present study was that of bending-torsion flutter of a wing with non-linear structural characteristics. Two aspects of non-linear systems were investigated, namely, amplitude limitation and stability dependence upon disturbance size.

Throughout the present study it was assumed that the non-linearities were small so that the physical system considered deviated only slightly from a corresponding linear one. The air speed was restricted to the range in which linear piston theory is applicable and airfoil thickness effects were neglected.

Several mathematical techniques are available for the approximate solution of vibration problems containing a small non-linearity, notably the famous Poincaré perturbation method, a variety of phase plane techniques, the method of slowly varying parameters, and the method of harmonic linearization. Except for the last two, the above methods are tedious if not impossible to apply to problems containing more than one degree of freedom. Of the last two, the method of harmonic linearization is the simplest to apply for the determination of limit cycles, but stability questions are only resolved through Mathieu-Hill techniques. For application to the study of both limit cycles and stability, therefore, the method of slowly varying parameters was employed. This is not to say that all of the tedium or algebraic difficulty is removed by the selection of this method. Quite the contrary! And in fact, some of the conclusions of the present study were obscured by excessive algebraic complication and recourse to some numerical examples was necessary. This, however, appears to be a typical shortcoming of all the existent techniques for solution of non-linear problems.

CHAPTER II

GENERAL FORMULATION

The problem considered here is that of bending-torsion oscillation of a wing, and in particular the self excited type of oscillation which is known as flutter. The occurrence of flutter requires, in general, two or more degrees of freedom (cf. ref. 1, p. 161). Exceptional situations arise in which one degree of freedom flutter occurs but these are associated with unusual elastic axis locations and their occurrence or non-occurrence is independent of the stiffness properties of the wing. In the present section the equations of motion for an oscillating wing will be set up and the method of finding limit cycle solutions outlined in general terms. Next, the method employed for investigating the stability of the limit cycles will be outlined, and finally, some comments on the dependence of the limit cycles upon initial conditions will be given.

2.0 Equations of Motion

It will be assumed in all of the analysis which follows that the bending-torsion flutter problem can be treated as a two-dimensional situation in which the structural resistance to bending can be represented by a single spring called the "bending spring" and that the structural resistance to twisting can be represented by a single spring called the "torsion spring". To complement this structural model, two-dimensional aerodynamics was assumed to apply. These assumptions are fundamental to what is commonly known as two-dimensional flutter theory. The aerodynamic assumptions are strictly applicable to three-dimensional wings of large aspect ratio only, but for the Mach number range presently under consideration they are satisfactory even for moderately low aspect ratios. This is true since at high supersonic speeds the flow over the wing is two-dimensional over all of the span except for a small region near the tip.

Figure 1 shows the coordinates and geometry of the two-dimensional airfoil.

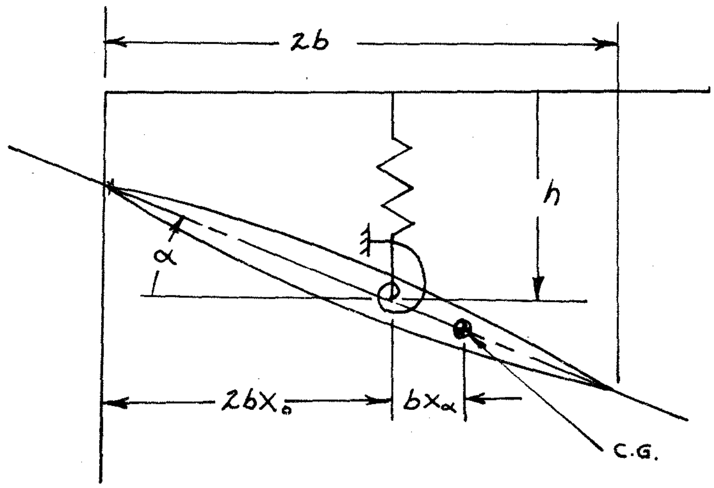

Figure 1

The application of Newton's second law of motion to the system of Figure 1, gives the following equations of motion:

$$m\ddot{h} + mbx_\alpha\ddot{\alpha} + hC_h = -L(t) \tag{2.1}$$

$$mbx_\alpha\ddot{h} + I_\alpha\ddot{\alpha} + \alpha C_\alpha = M(t) \tag{2.2}$$

where:

m = airfoil mass per unit span ($\frac{\text{lb sec}^2}{\text{ft}^2}$)

C_h = bending spring control function (lb/ft)

C_α = torsion spring control function (lb)

I_α = airfoil moment of inertia about the elastic axis (lb sec^2)

L(t) = aerodynamic lift per unit span, positive upward (lb/ft)

M(t) = aerodynamic moment per unit span about the elastic axis, positive nose down (lb)

It is convenient in prescribing the spring control functions to introduce the quantities ω_h , the natural frequency of the system constrained to have only bending deflection, and ω_α the natural frequency of the system constrained to have only torsional deflection. (Both at zero air speed.) In terms of these quantities the spring control terms can be written

$$C_h = m\omega_h^2\left[1 + \frac{\epsilon}{h}\bar{f}_1(h)\right] \tag{2.3}$$

$$C_\alpha = I_\alpha\omega_\alpha^2\left[1 + \frac{\epsilon}{\alpha}\bar{f}_2(\alpha)\right] \tag{2.4}$$

where

$\bar{f}_1(h)$ = the deviation from linearity of the bending spring

$\bar{f}_2(\alpha)$ = the deviation from linearity of the torsion spring

ϵ = a small constant

It is also convenient to introduce the airfoil pitching radius of gyration about the elastic axis, r_α . When this parameter is expressed in airfoil semi-chords the pitching moment of inertia is given by the relation

$$I_\alpha = m b^2 r_\alpha^2 \tag{2.5}$$

In this notation the equations of motion become:

$$m\ddot{h} + m b x_\alpha \ddot{\alpha} + m\omega_h^2 [h + \epsilon \bar{f}_1(h)] = -L(t) \tag{2.6}$$

$$m b x_\alpha \ddot{h} + m b^2 r_\alpha^2 \ddot{\alpha} + m b^2 r_\alpha^2 \omega_\alpha^2 [\alpha + \epsilon \bar{f}_2(\alpha)] = M(t) \tag{2.7}$$

These equations can be made non-dimensional by introducing the quantities

$$\tau = \frac{Ut}{b} \tag{2.8}$$

$$k = \frac{\omega b}{U} \tag{2.9}$$

$$X = \frac{\omega_\alpha^2}{\omega^2} \tag{2.10}$$

where

U = wing forward speed (ft/sec)

ω = frequency of vibration (rad/sec)

In this notation the equations of motion become

$$\frac{h''}{b} + k^2 X R\left[\frac{h}{b} + \epsilon f_1\left(\frac{h}{b}\right)\right] + x_\alpha \alpha'' = -\frac{b L(\tau)}{m U^2} \tag{2.11}$$

$$r_\alpha^2 \alpha'' + k^2 X r_\alpha^2 [\alpha + \epsilon f_2(\alpha)] + x_\alpha \frac{h''}{b} = \frac{M(\tau)}{m U^2} \tag{2.12}$$

where the primes indicate differentiation with respect to τ, and $R = \frac{\omega_h^2}{\omega_\alpha^2}$.

The aerodynamic forces are given by:

$$L(\tau) = 4 b \rho_\infty a_\infty^2 M\left[\frac{h'}{b} + \alpha + (1-2x_0)\alpha'\right] \tag{2.13}$$

$$M(\tau) = -4 b^2 \rho_\infty a_\infty^2 M\left[(1-2x_0)\left(\frac{h'}{b}+\alpha\right) + \left(\frac{4}{3} - 4x_0 + 4x_0^2\right)\alpha'\right] \tag{2.14}$$

where:

ρ_∞ = free stream air density (slugs/ft^3)

a_∞ = free stream speed of sound (ft/sec)

$M = \dfrac{U}{a_\infty}$ = free stream Mach number

X_0 = elastic axis location (Figure 1)

Then

$$\frac{-b L(\tau)}{m U^2} = -\lambda\left[\frac{h'}{b} + \alpha + P\alpha'\right] \tag{2.15}$$

$$\frac{M(\tau)}{m U^2} = -\lambda\left[\left(\frac{h'}{b}+\alpha\right)P + Q\alpha'\right] \tag{2.16}$$

where

$\mu = \dfrac{m}{4\rho b^2}$ = flutter mass ratio parameter

$\lambda = \dfrac{1}{\mu M}$

$P = 1 - 2x_0$

$Q = \dfrac{4}{3} - 4x_0 + 4x_0^2$

The final equations of motion are then

$$\frac{h''}{b} + k^2 \Xi R\left[\frac{h}{b} + \epsilon f_1\left(\frac{h}{b}\right)\right] + x_\alpha \alpha'' = -\lambda\left[\frac{h'}{b} + \alpha + \alpha' P\right] \tag{2.17}$$

$$r_\alpha^2 \alpha'' + k^2 \Xi r_\alpha^2\left[\alpha + \epsilon f_2(\alpha)\right] + x_\alpha \frac{h''}{b} = -\lambda\left[\left(\frac{h'}{b}+\alpha\right)P + \alpha' Q\right] \tag{2.18}$$

Equations 2.17 and 2.18 are in the form customarily used for linear flutter calculations. These, however, are not convenient for use in the method to be employed for the non-linear solution. The difficulty arises from the fact that the equations are mass coupled. This difficulty is easily circumvented by a transformation of the equations which removes the mass coupling terms. The first uncoupled equation is found by multiplying equation 2.17 by r_α^2, equation 2.18 by $(-x_\alpha)$ and adding the resulting pair of equations. The second uncoupled equation is obtained by multiplying equation 2.17 by $(-x_\alpha)$ and adding the result to equation 2.18. These operations give:

$$(r_\alpha^2 - x_\alpha^2)\frac{h''}{b} + k^2 r_\alpha^2 \left\{ R\bar{\Sigma}\left[\frac{h}{b} + \epsilon f_1\left(\frac{h}{b}\right)\right] - x_\alpha \bar{\Sigma}\left[\alpha + \epsilon f_2(\alpha)\right]\right\} = \lambda\left(\frac{h'}{b} + \alpha\right)(Px_\alpha - r_\alpha^2) + \lambda\alpha'(Px_\alpha - Q) \tag{2.19}$$

$$(r_\alpha^2 - x_\alpha^2)\alpha'' + k^2 r_\alpha^2 \left\{ \bar{\Sigma}\left(\alpha + \epsilon f_2(\alpha)\right) - \frac{x_\alpha}{r_\alpha^2} R\bar{\Sigma}\left[\frac{h}{b} + \epsilon f_1\left(\frac{h}{b}\right)\right]\right\} = \lambda\left(\frac{h'}{b} + \alpha\right)(x_\alpha - P) + \lambda\alpha'(Px_\alpha - Q) \tag{2.20}$$

These are the equations of motion for the flutter system which will be used throughout the present study.

2.1 Method of Solution

The method chosen for solution of equations 2.19 and 2.20 was the one known variously as "the method of slowly varying parameters", "the method of Kryloff and Bogoliuboff", and "the method of the mean". This method was first employed by N. Kryloff and N. Bogoliuboff and was published in Reference 2. This method has been used almost exclusively for the study of systems having only one degree of freedom although in at least two cases it has been successfully employed for the study of forced vibrations of systems having several degrees of freedom (Refs. 3 and 4).

The application of this method to the present problem is outlined below. Assume solutions to equations 2.19 and 2.20 in the form

$$\frac{h}{b} = \frac{h_o}{b}(\tau)\, SIN[K\tau + \varphi_1(\tau)] \tag{2.21}$$

$$\alpha = \alpha_o(\tau)\, SIN[K\tau + \varphi_2(\tau)] \tag{2.22}$$

where the amplitude and phase functions $\frac{h_o}{b}(\tau)$, $\alpha_o(\tau)$, $\varphi_1(\tau)$ and $\varphi_2(\tau)$ are all slowly varying functions of time. The meaning of slowly varying will be elaborated upon at a later state of the development.

If the amplitude and phase functions were in fact constants, first derivatives of equations 2.21 and 2.22 would be

$$\frac{h'}{b} = \frac{h_o}{b} K \cos(K\tau + \varphi_1) \tag{2.23}$$

$$\alpha' = \alpha_o K \cos(K\tau + \varphi_2) \tag{2.24}$$

whereas consideration of the time dependence of the amplitude and phase functions results in

$$\frac{h'}{b} = \frac{h_o'}{b} SIN(K\tau + \varphi_1) + \frac{h_o}{b}(K + \varphi_1')\cos(K\tau + \varphi_1) \tag{2.25}$$

$$\alpha' = \alpha_o' SIN(K\tau + \varphi_2) + \alpha_o(K + \varphi_2')\cos(K\tau + \varphi_2) \tag{2.26}$$

It is apparent that equations 2.23 and 2.24 can be used for the first derivatives provided that an auxiliary set of conditions is imposed on the system, namely:

$$\frac{h_o'}{b} \sin(\kappa\tau+\varphi_1) + \frac{h_o}{b}\varphi_1' \cos(\kappa\tau+\varphi_1) = 0 \tag{2.27}$$

$$\alpha_o' \sin(\kappa\tau+\varphi_2) + \alpha_o \varphi_2' \cos(\kappa\tau+\varphi_2) = 0 \tag{2.28}$$

Taking the derivatives with respect to time of equations 2.23 and 2.24 gives

$$\frac{h''}{b} = \kappa\frac{h_o'}{b} \cos(\kappa\tau+\varphi_1) - \frac{h_o}{b}\kappa(\kappa+\varphi_1') \sin(\kappa\tau+\varphi_1) \tag{2.29}$$

$$\alpha'' = \kappa\alpha_o' \cos(\kappa\tau+\varphi_2) - \alpha_o\kappa(\kappa+\varphi_2') \sin(\kappa\tau+\varphi_2) \tag{2.30}$$

Introducing the notation

$$\theta_1 = \kappa\tau + \varphi_1 \tag{2.31}$$

$$\theta_2 = \kappa\tau + \varphi_2 \tag{2.32}$$

and substituting equations 2.21, 2.22, 2.23, 2.24, 2.29 and 2.30 into equations 2.19 and 2.20 gives:

$$\begin{aligned}(r_\alpha^2 - x_\alpha^2)\left[\kappa\frac{h_o'}{b}\cos\theta_1 - \frac{h_o}{b}\kappa(\kappa+\varphi_1')\sin\theta_1\right] + \kappa r_\alpha^2\Big\{R\Xi\left[\frac{h_o}{b}\sin\theta_1 + \epsilon f_1\right] \\ - x_\alpha \Xi\left[\alpha_o \sin\theta_2 + \epsilon f_2\right]\Big\} = \lambda(Px_\alpha - r_\alpha^2)\left(\frac{h_o}{b}\kappa\cos\theta_1 + \alpha_o \sin\theta_2\right) \\ + \lambda(Qx_\alpha - Pr_\alpha^2)\alpha_o\kappa\cos\theta_2\end{aligned} \tag{2.33}$$

$$\begin{aligned}(r_\alpha^2 - x_\alpha^2)\left[\kappa\alpha_o'\cos\theta_2 - \alpha_o\kappa(\kappa+\varphi_2')\sin\theta_2\right] + \kappa^2 r_\alpha^2\Big\{\Xi\left[\alpha_o\sin\theta_2 + \epsilon f_2\right] \\ - \frac{x_\alpha}{r_\alpha^2} R\Xi\left[\frac{h_o}{b}\sin\theta_1 + \epsilon f_1\right]\Big\} = \lambda(x_\alpha - P)\left(\frac{h_o}{b}\kappa\cos\theta_1 + \alpha_o \sin\theta_2\right) \\ + \lambda(Px_\alpha - Q)\alpha_o\kappa\cos\theta_2\end{aligned} \tag{2.34}$$

Equations 2.33 and 2.34 together with the auxiliary equations 2.27 and 2.28 form a system of four simultaneous first order differential equations in the variables $\frac{h_0}{b}$, α_0, φ_1 and φ_2. By algebraic manipulation the system can be rewritten in the more convenient form:

$$K\beta^2 \frac{h_0'}{b} = \Big[A\frac{h_0}{b}\sin\theta_1 + B\frac{h_0}{b}\cos\theta_1 + C\alpha_0\sin\theta_2 + D\alpha_0\cos\theta_2 + \epsilon K^2 \bar{X} r_\alpha^2 (x_\alpha f_2 - R f_1)\Big]\cos\theta_1 \tag{2.35}$$

$$K\beta^2 \alpha_0' = \Big[E\frac{h_0}{b}\sin\theta_1 + F\frac{h_0}{b}\cos\theta_1 + G\alpha_0\sin\theta_2 + H\alpha_0\cos\theta_2 - \epsilon K^2 \bar{X} r_\alpha^2 \Big(f_2 - R\frac{x_\alpha}{r_\alpha^2} f_1\Big)\Big]\cos\theta_2 \tag{2.36}$$

$$-K\beta^2 \frac{h_0}{b}\varphi_1' = \Big[A\frac{h_0}{b}\sin\theta_1 + B\frac{h_0}{b}\cos\theta_2 + C\alpha_0\sin\theta_2 + D\alpha_0\cos\theta_2 + \epsilon K^2 \bar{X} r_\alpha^2 (x_\alpha f_2 - R f_1)\Big]\sin\theta_1 \tag{2.37}$$

$$-K\beta^2 \alpha_0\varphi_2' = \Big[E\frac{h_0}{b}\sin\theta_1 + F\frac{h_0}{b}\cos\theta_1 + G\alpha_0\sin\theta_2 + H\alpha_0\cos\theta_2 - \epsilon K^2 \bar{X} r_\alpha^2 \Big(f_2 - R\frac{x_\alpha}{r_\alpha^2} f_1\Big)\Big]\sin\theta_2 \tag{2.38}$$

where, due to the obvious need for compressed representation, the following notation has been employed:

$$
\begin{aligned}
p^2 &= (r_\alpha^2 - x_\alpha^2) & E &= \kappa^2 \overline{\underline{X}} R x_\alpha \\
A &= \kappa^2 (p^2 - r_\alpha^2 R \overline{\underline{X}}) & F &= \lambda\kappa (x_\alpha - P) \\
B &= \lambda\kappa (P x_\alpha - r_\alpha^2) & G &= \kappa^2 (p^2 - r_\alpha^2 \overline{\underline{X}}) + \lambda (x_\alpha - P) \\
C &= \kappa^2 \overline{\underline{X}} r_\alpha^2 x_\alpha + \lambda (P x_\alpha - r_\alpha^2) & H &= \lambda\kappa (P x_\alpha - Q) \\
D &= \lambda\kappa (Q x_\alpha - P r_\alpha^2) & &
\end{aligned}
$$

Equations 2. 35 through 2. 38 are exact, that is to say no approximations have yet been made. Up to this point in the development the procedure has been aimed simply toward a reformulation of the equations of motion. These originally took the form of two second order differential equations in the variables $h(\tau)$ and $\alpha(\tau)$ and in equations 2. 35 through 2. 38 have been transformed into four first order equations in the more convenient variables $h_0(\tau)$, $\alpha_0(\tau)$, $\varphi_1(\tau)$ and $\varphi_2(\tau)$. The Kryloff and Bogolouboff assumption of slowly varying amplitudes and phase angles can now be utilized to arrive at a first approximation to the solution of equations 2. 19 and 2. 20.

Since the quantities $\frac{h_0'}{b}$, α_0', φ_1' and φ_2' were assumed to be small, their percentage changes per cycle must be assumed small, that is to say of order ϵ. Thus, to the first order in ϵ, the quantities $\frac{h_0'}{b}$, α_0', φ_1' and φ_2' can be replaced by their averages over one cycle of motion, and for the purpose of computing these averages the quantities $\frac{h_0}{b}$, α_0, φ_1 and φ_2 may be assumed to be constant over a single cycle. It will be noted that the right hand sides of equations 2. 35 through 2. 38 all have a period of 2π in θ. Thus for the first order approximation we have

$$2\kappa p^2 \frac{h_o'}{b} = \frac{1}{\pi}\int_0^{2\pi} \ell_1(---)\cos\theta_1\, d\theta_1 = I_1\left(\frac{h_o}{b}, \alpha_o, \varphi_1, \varphi_2\right) \qquad (2.39)$$

$$2\kappa p^2 \alpha_o' = \frac{1}{\pi}\int_0^{2\pi} \ell_2(---)\cos\theta_2\, d\theta_2 = I_2\left(\frac{h_o}{b}, \alpha_o, \varphi_1, \varphi_2\right) \qquad (2.40)$$

$$-2\kappa p^2 \frac{h_o}{b}\varphi_1' = \frac{1}{\pi}\int_0^{2\pi} \ell_1(---)\sin\theta_1\, d\theta_1 = I_3\left(\frac{h_o}{b}, \alpha_o, \varphi_1, \varphi_2\right) \qquad (2.41)$$

$$-2\kappa p^2 \alpha_o \varphi_2' = \frac{1}{\pi}\int_0^{2\pi} \ell_2(---)\sin\theta_2\, d\theta_2 = I_4\left(\frac{h_o}{b}, \alpha_o, \varphi_1, \varphi_2\right) \qquad (2.42)$$

where:

$$\ell_1(---) = A\frac{h_o}{b}\sin\theta_1 + B\frac{h_o}{b}\cos\theta_1 + C\alpha_o\sin\theta_2 + D\alpha_o\cos\theta_2 + \epsilon K^2 \Sigma r_\alpha^2 (x_\alpha f_2 - R f_1)$$

$$\ell_2(---) = E\frac{h_o}{b}\sin\theta_1 + F\frac{h_o}{b}\cos\theta_1 + G\alpha_o\sin\theta_2 + H\alpha_o\cos\theta_2 - \epsilon K^2 \Sigma r_\alpha^2 \left(f_2 - R\frac{x_\alpha}{r_\alpha^2} f_1\right)$$

Performing the integration, the following result is obtained:

$$I_1 = B\frac{h_o}{b} + \left\{D\cos\varphi - [C + \mu(\alpha_o)x_\alpha]\sin\varphi\right\}\alpha_o \qquad (2.43)$$

$$I_2 = \left\{\left[E + \nu\left(\frac{h_o}{b}\right)x_\alpha\right]\sin\varphi + F\cos\varphi\right\}\frac{h_o}{b} + H\alpha_o \qquad (2.44)$$

$$I_3 = \left[A - \nu\left(\frac{h_o}{b}\right)r_\alpha^2\right]\frac{h_o}{b} + \left\{[C + \mu(\alpha_o)x_\alpha]\cos\varphi + D\sin\varphi\right\}\alpha_o \qquad (2.45)$$

$$I_4 = \left\{\left[E + \nu\left(\frac{h_o}{b}\right)x_\alpha\right]\cos\varphi - F\sin\varphi\right\}\frac{h_o}{b} + [G - \mu(\alpha_o)]\alpha_o \qquad (2.46)$$

where

$$\mu(\alpha_0) = \frac{\epsilon K^2 \overline{X} r_2^2}{\pi \alpha_0} \int_0^{2\pi} f_2(\alpha_0 \sin\theta_2) \sin\theta_2 \, d\theta_2$$

$$= \epsilon K^2 \overline{X} r_2^2 \, g_2(\alpha_0)$$

$$\nu\left(\frac{h_0}{b}\right) = \frac{\epsilon K^2 \overline{X} R}{\pi \frac{h_0}{b}} \int_0^{2\pi} f_1\left(\frac{h_0}{b} \sin\theta_1\right) \sin\theta_1 \, d\theta_1$$

$$= \epsilon K^2 \overline{X} R \, g_1\left(\frac{h_0}{b}\right)$$

The equations of motion have thus been reduced to

$$2K p^2 \frac{h_0'}{b} = I_1 \tag{2.47}$$

$$2K p^2 \alpha_0' = I_2 \tag{2.48}$$

$$-2K p^2 \frac{h_0}{b} \varphi_1' = I_3 \tag{2.49}$$

$$-2K p^2 \alpha_0 \varphi_2' = I_4 \tag{2.50}$$

The steady state solutions to equations 2.47 through 2.50 are obtained by setting $\frac{h_0'}{b}$, α_0', φ_1' and φ_2' all equal to zero. The resulting set of equations is a set of four non-linear algebraic equations in the five unknowns $\frac{h_0}{b}$, α_0, φ, K and $\overline{X}$. From these equations four of the unknowns can be solved for in terms of the fifth unknown. The existence of bounded solutions to these equations implies the existence of flutter limit cycles. The stability of the limit cycle solutions is determined from equations 2.47 through 2.50. It should be noted that the steady state solutions are dependent upon the phase difference, φ , between the bending and torsion displacements but not upon the separate phase angles, φ_1 , and φ_2 . This is apparent from the fact that the right hand sides of equations 2.47 through 2.50 contain only the phase difference, φ . This fact is not surprising since the steady state behavior was determined without reference to a time origin. Had the steady state solutions been found as functions of specified initial conditions, the separate phase angles would retain their significance. The disappearance of one phase angle suggests that the order of the system of equations determining the stability of the motion can be reduced by one. This is accomplished by multiplying equation 2.50 by $\frac{h_o}{b}$ and subtracting the result from α_o times equation 2.49. The resulting set of equations is

$$2k\beta^2 \frac{h_o'}{b} = I_1 \tag{2.51}$$

$$2k\beta^2 \alpha_o' = I_2 \tag{2.52}$$

$$-2k\beta^2 \alpha_o \frac{h_o}{b} \varphi' = I_5 \tag{2.53}$$

where

$$I_5 = \alpha_o I_3 - \frac{h_o}{b} I_4$$

Let the steady state solutions be denoted by $\overline{\frac{h_o}{b}}$, $\bar{\alpha}_o$ and $\bar{\varphi}$. The stability of these steady state solutions can now be found from equations 2.51 through 2.53. Let each of the solutions be perturbed from the steady state by a small amount.

$$\frac{h_o}{b} = \overline{\frac{h_o}{b}} + \xi_1 \tag{2.54}$$

$$\alpha_o = \bar{\alpha}_o + \xi_2 \tag{2.55}$$

$$\varphi = \bar{\varphi} + \eta_1 \tag{2.56}$$

The solutions are considered stable provided the perturbations die out or at least remain constant with increasing time. Substituting equations 2.54 through 2.56 into equations 2.51 through 2.53 and neglecting powers of ξ_1, ξ_2 and η_1 higher than the first gives:

$$2\kappa p^2 \xi_1' = \frac{\partial I_1}{\partial \frac{h_o}{b}} \xi_1 + \frac{\partial I_1}{\partial \alpha_o} \xi_2 + \frac{\partial I_1}{\partial \varphi} \eta_1 \tag{2.57}$$

$$2\kappa p^2 \xi_2' = \frac{\partial I_2}{\partial \frac{h_o}{b}} \xi_1 + \frac{\partial I_2}{\partial \alpha_o} \xi_2 + \frac{\partial I_2}{\partial \varphi} \eta_1 \tag{2.58}$$

$$2\kappa p^2 \eta_1' \alpha_o \frac{h_o}{b} = \frac{\partial I_5}{\partial \frac{h_o}{b}} \xi_1 + \frac{\partial I_5}{\partial \alpha_o} \xi_2 + \frac{\partial I_5}{\partial \varphi} \eta_1 \tag{2.59}$$

Equations 2.57 through 2.59 are a set of three simultaneous, linear, first order differential equations and admit solutions of the form $e^{\Omega\tau}$. The condition for a non-trivial solution of these equations is then:

$$\begin{vmatrix} \left(\frac{\partial I_1}{\partial \frac{h_o}{b}} - 2\kappa p^2 \Omega\right) & \frac{\partial I_1}{\partial \alpha_o} & \frac{\partial I_1}{\partial \varphi} \\ \frac{\partial I_2}{\partial \frac{h_o}{b}} & \left(\frac{\partial I_2}{\partial \alpha_o} - 2\kappa p^2 \Omega\right) & \frac{\partial I_2}{\partial \varphi} \\ \frac{\partial I_5}{\partial \frac{h_o}{b}} & \frac{\partial I_5}{\partial \alpha_o} & \left(\frac{\partial I_5}{\partial \varphi} + 2\kappa p^2 \alpha_o \frac{h_o}{b} \Omega\right) \end{vmatrix} = 0 \tag{2.60}$$

Expansion of this determinant gives the characteristic polynomial of the system:

$$(2\kappa\beta^2\Omega)^3 + a_2(2\kappa\beta^2\Omega)^2 + a_1(2\kappa\beta^2\Omega) + a_0 = 0 \tag{2.61}$$

The condition for stability is then that equation 2.61 have no roots with positive real parts, and this can be ascertained through application of the Routh-Hurwitz criteria for the cubic polynomial, namely

$$2\kappa\beta^2 \geq 0 \tag{2.62}$$

$$a_2 \geq 0 \tag{2.63}$$

$$a_1 \geq 0 \tag{2.64}$$

$$a_0 \geq 0 \tag{2.65}$$

$$a_2 a_1 \geq a_0 \tag{2.66}$$

A significant general conclusion can be drawn from one of these criteria, specifically equation 2.65, without treating the entire problem. The constant term, a_0 , is given by

$$a_0 = \begin{vmatrix} \frac{\partial I_1}{\partial \frac{h_0}{b}} & \frac{\partial I_1}{\partial \alpha_0} & \frac{\partial I_1}{\partial \varphi} \\ \frac{\partial I_2}{\partial \frac{h_0}{b}} & \frac{\partial I_2}{\partial \alpha_0} & \frac{\partial I_2}{\partial \varphi} \\ \frac{\partial I_5}{\partial \frac{h_0}{b}} & \frac{\partial I_5}{\partial \alpha_0} & \frac{\partial I_5}{\partial \varphi} \end{vmatrix} = \frac{\partial(I_1, I_2, I_5)}{\partial(\frac{h_0}{b}, \alpha_0, \varphi)} \tag{2.67}$$

For the steady state

$$I_1 = I_2 = I_3 = I_4 = I_5 = 0, \tag{2.68}$$

but the I's are all functions of the flutter parameters k, and x. Thus by the usual formulas for parametric partial derivatives,

$$\frac{\partial \frac{h_o}{b}}{\partial K} = - \frac{\frac{\partial(I_1, I_2, I_5)}{\partial(K, \alpha_o, \varphi)}}{\frac{\partial(I_1, I_2, I_5)}{\partial(\frac{h_o}{b}, \alpha_o, \varphi)}} = - \frac{\frac{\partial(I_1, I_2, I_5)}{\partial(K, \alpha_o, \varphi)}}{a_o} \tag{2.69}$$

$$\frac{\partial \frac{h_o}{b}}{\partial X} = - \frac{\frac{\partial(I_1, I_2, I_5)}{\partial(X, \alpha_o, \varphi)}}{a_o} \tag{2.70}$$

$$\frac{\partial \alpha_o}{\partial K} = - \frac{\frac{\partial(I_1, I_2, I_5)}{\partial(K, \frac{h_o}{b}, \varphi)}}{a_o} \tag{2.71}$$

$$\frac{\partial \alpha_o}{\partial X} = - \frac{\frac{\partial(I_1, I_2, I_5)}{\partial(X, \frac{h_o}{b}, \varphi)}}{a_o} \tag{2.72}$$

But by equation 2.65 a sufficient condition for instability is $a_o < 0$. Thus it can be concluded that $a_o = 0$ is a point of neutral stability and except for special cases a point of transition from stability to instability or vice versa. But from equations 2.69 through 2.72 it can be seen that $a_o = 0$ represents points of vertical tangency on plots of amplitude versus both of the flutter parameters k and x. From this fact and from the definitions of k and x it can then be concluded that these are also points of vertical tangency on plots of amplitude versus flutter speed. Thus in the treatment to follow, considerable attention will be given to the existence of these vertical tangents whenever questions of stability are involved. Unfortunately the vertical tangents only provide sufficient conditions for stability transitions and the determination of both necessary and sufficient conditions requires consideration of the complete system of Routh-Hurwitz criteria and thus a consideration of all the parameters in the flutter system.

CHAPTER III

SPECIFIC ANALYTICAL SOLUTIONS

In this section a linear flutter system which will have later pertinence to the problem of non-linear flutter is introduced. It is shown that certain aerodynamic simplifications can be introduced into the linear system without materially affecting the flutter results. A brief discussion is then given of the mechanism of bending-torsion flutter.

Next, a non-linear flutter system similar to the simplified linear system is discussed and completely solved. The existence and stability of the flutter limit cycles for this system is then investigated. Finally, the complete non-linear system is investigated, limit cycle solutions are found, and stability criteria are developed. The results for the complete system are then interpreted in the light of the results obtained for the simplified system.

3.0 An Examination of the Linear Case

Before treating the non-linear bending-torsion flutter problem it will be found useful to examine the corresponding linear problem. The particular value of this examination lies in the determination of the relative magnitudes of certain of the physical parameters and in the suggestion of a simplified approximation. It will be found that this information is of value in the subsequent non-linear analysis.

The equations of motion for the linear system are obtained by setting the parameter, ϵ , equal to zero in equations 2.17 and 2.18. This gives

$$\frac{h''}{b} + K^2 \Sigma \mathcal{R} \frac{h}{b} + x_\alpha \alpha'' = -\lambda \left[\frac{h'}{b} + \alpha + \alpha' P \right] \tag{3.1}$$

$$r_\alpha^2 \alpha'' + K^2 \Sigma r_\alpha^2 \alpha + x_\alpha \frac{h''}{b} = -\lambda \left[\left(\frac{h'}{b} + \alpha \right) P + \alpha' Q \right] \tag{3.2}$$

The system defined by equations 3.1 and 3.2 will, in general exhibit two aeroelastic modes of motion. Each mode will have associated with it a characteristic frequency and rate of damping. The frequencies and damping rates will be dependent upon the airspeed as is indicated by the appearance in the equations of the parameters $K^2\Sigma$ and λ. If the characteristic frequencies and damping rates associated with the modes are determined for various values of the airspeed it will be found that below a certain critical value of the airspeed both of the system modes exhibit positive damping. At the critical value of airspeed the damping in one of the modes vanishes while the other damping rate remains positive. For values of the airspeed greater than the critical value the damping in one of the modes becomes negative while the other mode remains positively damped. This critical airspeed is called the flutter speed. The flutter speed for this linear system is easily obtained since it corresponds to a situation in which the set of equations 3.1 and 3.2 should exhibit a steady state behavior consisting of a single mode of undamped sinusoidal motion, the motion in the other mode having vanished due to its positive damping. Under these conditions, equations 3.1 and 3.2 will admit solutions in the form

$$\frac{h}{b} = \frac{h_o}{b} e^{ik\tau} \tag{3.3}$$

$$\alpha = \alpha_o e^{ik\tau} \tag{3.4}$$

where $\frac{h_o}{b}$ and α_o are complex amplitudes. When equations 3.3 and 3.4 are substituted into equations 3.1 and 3.2 and the resulting pair of real and imaginary equations are solved there results

$$k^2 X = \frac{\omega_\alpha^2 b^2}{U^2} = \frac{\lambda X\left[P(1-RX) - x_\alpha\right] + \lambda^2 (Q - P^2) X}{r_\alpha^2 (1-X)(1-RX) - x_\alpha^2} \tag{3.6}$$

$$X = \frac{\omega_\alpha^2}{\omega^2} = \frac{-2Px_\alpha + Q + r_\alpha^2}{RQ + r_\alpha^2} \tag{3.7}$$

This completely solves the problem of determining the flutter speed and frequency for the linear case. If, however, it is desired to determine the system behavior in the transient sense and thus to examine its characteristics at speeds other than the flutter speed it becomes necessary to account in the assumed solution for the presence of two modal frequencies and damping rates. This is done by assuming in place of equations 3.3 and 3.4 that

$$\alpha = \alpha_o e^{\Omega\tau} \tag{3.8}$$

$$\frac{h}{b} = \frac{h_o}{b} e^{\Omega\tau} \tag{3.9}$$

where, now, $\frac{h_o}{b}$ and α_o are complex constants and Ω is complex as well. When these solutions are substituted into the equations of motion the following quartic polynomial is obtained:

$$\begin{aligned} &\gamma^2\Omega^4 + \Omega^3\left[\lambda\left(-2Px_\alpha + Q + r_\alpha^2\right)\right] + \Omega^2\left[r_\alpha^2 k^2 \underline{X}(1+R) + \lambda(P - x_\alpha)\right. \\ &\left.+\lambda^2(Q - P^2)\right] + \Omega\left\{\lambda\left[k^2\underline{X}\left(r_\alpha^2 + QR\right)\right]\right\} + Rk^2\underline{X}\left(r_\alpha^2 k^2 \underline{X} + \lambda P\right) = 0 \end{aligned} \tag{3.10}$$

While the general solution to this quartic polynomial can be found, the results would not justify the tedium involved in obtaining such a solution. Instead, for the purposes at hand, a specific numerical solution to equation 3.10 will be given. The parameters chosen for the example are

$$\begin{aligned} R &= 0.500 \\ \mu &= 15.708 \\ r_\alpha^2 &= 0.250 \\ x_\alpha &= 0.200 \\ P &= 0.200 \\ Q &= 0.333 \\ a &= 1000 \text{ ft/sec} \\ \omega_\alpha^2 b^2 &= 1.2462 \times 10^6 \text{ ft}^2/\text{sec}^2 \end{aligned}$$

The airspeed, U , is varied from 3000 to 7000 feet per second.

When the above values are substituted into equation 3.10 it is found that, in general, the roots occur in conjugate complex pairs:

$$\Omega_{1,2} = \bar{a} \pm i\bar{b} \tag{3.11}$$

$$\Omega_{3,4} = \bar{c} \pm i\bar{d} \tag{3.12}$$

When equations 3.11 and 3.12 are substituted into equations 3.8 and 3.9 it is found that the roots are related to the frequency and damping of the transient solution by

$$\frac{h}{b}, \alpha \sim e^{\frac{\bar{a}U\tau}{b}}\left(C_1 \sin \frac{\bar{b}U\tau}{b} + C_2 \cos \frac{\bar{b}U\tau}{b}\right) + e^{\frac{\bar{c}U\tau}{b}}\left(C_3 \sin \frac{\bar{d}U\tau}{b} + C_4 \cos \frac{\bar{d}U\tau}{b}\right) \tag{3.13}$$

The constants C_1 through C_4 give only the amplitudes of the motion and are dependent upon the method of excitation of the airfoil, i.e. the initial conditions, but it can be seen that both the frequency and damping are completely determined by the roots of equations 3.11 and 3.12.

The results of finding the roots for the numerical example are shown plotted in Figure 2. Here the independent variable, the airspeed U , is plotted versus both dimensionless frequency and damping coefficient. It can be seen that the previously mentioned transient characteristics of the system are present; namely, the occurrence of two distinct aeroelastic modes of vibration and the existence of a critical speed below which both modes are positively damped, and above which one of the modes is negatively damped. For the example chosen, the critical speed is 5000 feet per second.

An interesting secondary observation can be made from Figure 2. This is the apparent tendency of the modal frequencies to approach each other as the airspeed is increased. This phenomenon is one which has been recognized by flutter engineers for many years and is, in fact, the basis for a method of flight flutter testing in which the separation of transient frequencies is observed as an index to the onset of flutter. It should be noted, however, that the occurrence of flutter

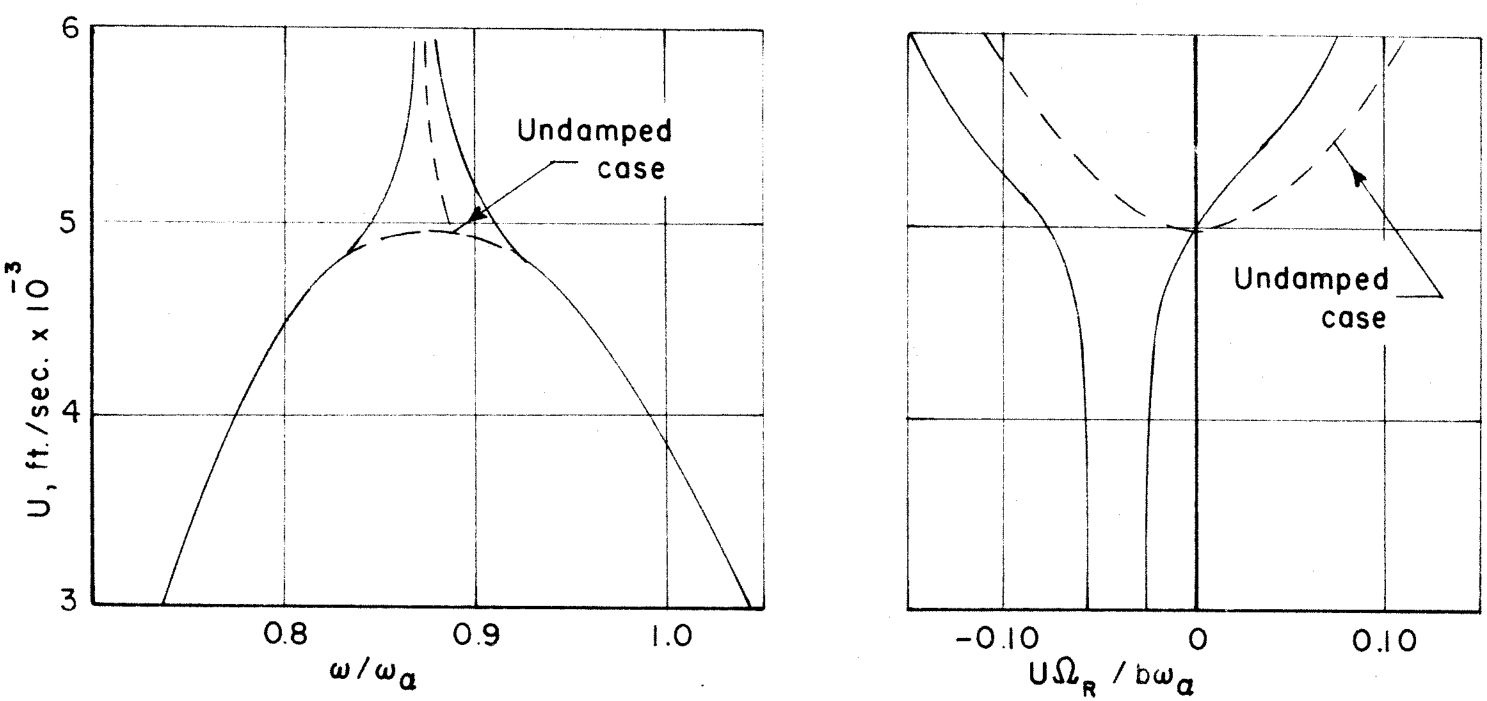

(a) (b)

FIG. 2a, 2b AIRSPEED VERSUS DIMENSIONLESS FREQUENCY AND DAMPING is not accompanied by an actual coalescence of the two frequencies. This fact is often overlooked and it will be found useful to expand the idea of frequency separation for later application to the non-linear flutter problem.

The magnitude of the frequency separation can be determined analytically from equation 3.10 when the airspeed is exactly equal to the flutter speed. This is done by observing that at the flutter speed one of the reduced frequencies is given by equations 3.6 and 3.7. This implies that

$$\bar{a} = 0 \tag{3.14}$$

$$\bar{b} = \kappa \tag{3.15}$$

and hence

$$\Omega_{1,2} = \pm i\kappa \tag{3.16}$$

The remaining pair of roots must then satisfy the quadratic equation which results from factoring out $\pm$ ik from equation 3.10. This quadratic is

$$\beta^2\Omega^2 + \Omega[\lambda(-2Px_\alpha + Q + r_\alpha^2)] + [r_\alpha^2\kappa^2\overline{\underline{X}}(1+R) + \lambda(P - x_\alpha) + \lambda^2(Q - P^2) - \beta^2\kappa] = 0 \tag{3.17}$$

from which

$$\Omega_{3,4} = \frac{-\lambda}{2\beta^2}(-2Px_\alpha + Q + r_\alpha^2) \pm \frac{1}{2\beta^2}\left\{\lambda^2(-2Px_\alpha + Q + r_\alpha^2)^2 - 4\beta^2[r_\alpha^2\kappa^2\overline{\underline{X}}(1+R) + \lambda(P - x_\alpha) + \lambda^2(Q - P^2) - \beta^2\kappa^2]\right\}^{1/2} \tag{3.18}$$

Comparing this with equation 3.12 gives

$$\bar{c} = -\frac{\lambda(-2Px_\alpha + Q + r_\alpha^2)}{2\wp^2} \tag{3.19}$$

$$\bar{d} = \frac{1}{2\wp^2}\Big\{4\wp^2\left[r_\alpha^2 K^2 \overline{X}(1+R) + \lambda(P - x_\alpha) + \lambda^2(Q - P^2) - \wp^2 K\right] - \lambda^2(-2Px_\alpha + Q + r_\alpha^2)^2\Big\}^{1/2} \tag{3.20}$$

As previously noted, the quantity $\bar{c}$ gives the damping rate associated with the non-fluttering mode while $\bar{d}$ gives the corresponding frequency. The frequency separation can then be determined from equations 3.6, 3.7 and 3.20. For the present purposes the difference, Δ, in the squares of the two frequencies will be computed.

$$\Delta = \bar{d}^2 - K^2 \tag{3.22}$$

or, substituting from equation 3.20

$$\wp^2\Delta = r_\alpha^2 K^2 \overline{X}(1+R) + \lambda(P - x_\alpha) - 2\wp^2 K^2 + \lambda^2(Q - P^2) - \frac{\lambda^2}{4\wp^2}(-2Px_\alpha + Q + r_\alpha^2)^2 \tag{3.23}$$

This expression will be useful in the discussion which follows.

To complete the discussion of the linear system it will be necessary to consider briefly the case of flutter of an airfoil in which the aerodynamic damping is sufficiently small to be negligible. The equations of motion for this case are

$$\frac{h''}{b} + RK^2\overline{X}\,\frac{h}{b} + x_\alpha \alpha'' = -\lambda\alpha \tag{3.24}$$

$$r_\alpha^2\alpha'' + r_\alpha^2 K^2 \overline{X}\alpha + x_\alpha \frac{h''}{b} = -\lambda P\alpha \tag{3.25}$$

The characteristic equation for this system, obtained in a manner identical with that used to obtain equation 3.10 is

$$\gamma^2\Omega^4 + \Omega^2\left[r_\alpha^2 K^2\overline{X}(1+R) + \lambda(P - x_\alpha)\right] + RK^2\overline{X}\left(r_\alpha^2 K^2 \overline{X} + \lambda P\right) = 0 \tag{3.26}$$

The roots of this equation determine the modal frequencies and damping rates as before. These are shown plotted in Figure 2 for the same numerical case as was used for the aerodynamically damped system. It can be seen from Figure 2 that while the general behavior of the undamped or aerodynamically conservative system is different from that of the damped case, a number of its essential features are retained. As would be expected, the aerodynamically conservative system exhibits sinusoidal motion in each of its modes for all airspeeds below a certain critical airspeed. There does exist, however, a value of airspeed, above which the system exhibits a positively damped motion in one aeroelastic mode while exhibiting negative damping in the other. Thus, it might be said that the undamped system possesses a "flutter" speed, provided that this speed is defined as the largest value of airspeed at which undamped sinusoidal oscillation can be maintained. A comparison of the plots shown in Figure 2 indicates that the two flutter speeds are in very close agreement, and that the neglect of aerodynamic damping results in a slightly conservative estimate of the flutter speed.

The variation of frequency with airspeed for the undamped system can be determined quite simply from equation 3.26 by setting $\Omega = \pm i\kappa$ and solving for $\kappa^2 X$. This gives

$$\kappa^2 X = \frac{\omega_\alpha^2 b^2}{U^2} = \frac{\lambda X\left[P(1-RX)-x_\alpha\right]}{r_\alpha^2(1-X)(1-RX)-x_\alpha^2} \tag{3.27}$$

The value of X corresponding to flutter can be obtained from equation 3.27 by minimizing $\kappa^2 X$ with respect to X and solving the result for X. The result is a bit cumbersome to use, however, and will not be shown here. A comparison of equation 3.27 with equation 3.6 reveals that the two systems show identical variation of frequency with airspeed except for the term $\lambda^2(Q-P^2)X$. The portion of this expression given by $(Q-P^2)X$ must be finite for flutter to exist as is evident from the definitions of the symbols themselves, and thus it can be concluded that the only parameter in this expression which can be freely varied is the term λ^2. Consequently it can be concluded that the attainment of good agreement between the results of the aerodynamically conservative analysis and the more exact analysis depends upon the smallness of the parameter λ^2. For compatibility with the non-linear analysis this condition will be expressed as

$$\lambda^2 = O(\epsilon) \tag{3.28}$$

where ϵ is the small parameter previously identified with the non-linear spring terms.

Examination of the frequency curve for the passive case in Figure 2 shows that the modal frequencies do in fact coalesce at the flutter speed. This leads to the conclusion that the degree of frequency separation depends upon the magnitude of the aerodynamic damping and thus upon the magnitude of the parameter λ^2 . If equation 3.28 is substituted into the equation for the frequency separation 3.23 the result is

$$\beta^2\Delta = r_\alpha^2 k^2 \bar{X}(1+R) + \lambda(P-x_\alpha) - 2\beta^2 k^2 + O(\epsilon) \tag{3.29}$$

If it is assumed that the frequency separation is itself of order ϵ , equation 3.29 becomes

$$r_\alpha^2 k^2 \bar{X}(1+R) + \lambda(P-x_\alpha) - 2\beta^2 k^2 = O(\epsilon) \tag{3.30}$$

This can be rewritten in the notation of section 2 as

$$A + G = O(\epsilon) \tag{3.31}$$

In all of the analysis which follows the assumption will be made that the aerodynamic damping and thus the frequency separation is small.

3.1 A Simplified Non-linear Case

It was shown in the preceding section that the neglect of damping in the aerodynamic representation gives flutter results which are in good agreement with more exact aerodynamic theory. It thus seems probable that the same representation would give a good approximation to the flutter behavior of the structurally non-linear case providing the non-linearities are small.

For simplicity of presentation in this section the structural non-linearity has been limited to the torsional degree of freedom. Under this restriction and neglecting aerodynamic damping the equations of motion are obtained by setting the function $f_1\left(\frac{h_0}{b}\right)$ and all first order time derivatives equal to zero in equations 2.19 and 2.20 to give

$$p^2\frac{h''}{b} + K^2 r_\alpha^2\left\{R\Xi\frac{h}{b} - x_\alpha\Xi\left[\alpha + \epsilon f_2(\alpha)\right]\right\} = \lambda\alpha\left(Px_\alpha - r_\alpha^2\right) \tag{3.32}$$

$$p^2\alpha'' + K^2 r_\alpha^2\left\{\left[\alpha + \epsilon f_2(\alpha)\right]\Xi - \frac{x_\alpha}{r_\alpha^2}R\Xi\frac{h}{b}\right\} = \lambda\alpha\left(x_\alpha - P\right) \tag{3.33}$$

Following the method of section 2.1 the equations of motion can be reduced to the four first order differential equations:

$$2Kp^2\frac{h_0'}{b} = -\left\{(C+\mu x_\alpha)\sin\varphi\right\}\alpha_0 \tag{3.34}$$

$$2Kp^2\alpha_0' = (E\sin\varphi)\frac{h_0}{b} \tag{3.35}$$

$$-2Kp^2\frac{h_0}{b}\varphi_1' = A\frac{h_0}{b} + \alpha_0(C+\mu x_\alpha)\cos\varphi \tag{3.36}$$

$$-2Kp^2\alpha_0\varphi_2' = (E\cos\varphi)\frac{h_0}{b} + \alpha_0(G-\mu) \tag{3.37}$$

where the notation of section 2.1 has been retained.

Steady state solutions are obtained by setting $\frac{h_0'}{b}$, α_0', φ_1' and φ_2' all equal to zero to give

$$\alpha_0 (C + \mu x_\alpha) \sin\varphi = 0 \tag{3.38}$$

$$\frac{h_0}{b}(E \sin\varphi) = 0 \tag{3.39}$$

$$\frac{h_0}{b} A + \alpha_0 (C + \mu x_\alpha) \cos\varphi = 0 \tag{3.40}$$

$$\frac{h_0}{b}(E \cos\varphi) + \alpha_0 (G - \mu) = 0 \tag{3.41}$$

From equations 3.38 and 3.39 it is seen that

$$\sin\varphi = 0 \tag{3.42}$$

thus $\varphi = 0$ or π. Taking $\varphi = 0$ equations 3.40 and 3.41 become

$$\frac{h_0}{b} A + \alpha_0 (C + \mu x_\alpha) = 0 \tag{3.43}$$

$$\frac{h_0}{b} E + \alpha_0 (G - \mu) = 0 \tag{3.44}$$

Eliminating α_0 and $\frac{h_0}{b}$ from these equations gives

$$A(G - \mu) = E(C + \mu x_\alpha) \tag{3.45}$$

This, in compressed notation is the equation which relates airspeed with the frequency of motion. This fact can be seen more clearly by returning to the conventional flutter notation and solving equation 3.45 for the reduced frequency to give

$$k^2 \overline{\underline{X}} = \frac{\lambda \left[P(1 - R\overline{\underline{X}}) - x_\alpha \right] \overline{\underline{X}}}{r_\alpha^2 (1 - R\overline{\underline{X}}) \left[1 - \overline{\underline{X}} (1 + g_2(\alpha_0)) \right] - x_\alpha^2} \tag{3.46}$$

It can be seen from the appearance of the function $g_2(\alpha_0)$ in equation 3.46 that the non-linearity has caused the airspeed frequency relationship to be dependent upon the amplitude of torsional motion, α_0, and that except for this term equation 3.46 is identical with equation 3.27.

At this point the results obtained can best be demonstrated through a numerical example. To accomplish this a specific non-linearity must be chosen and it will be found that the type best suited to this end is that of a "soft-hard" torsion spring whose characteristics are shown in Figure 3.

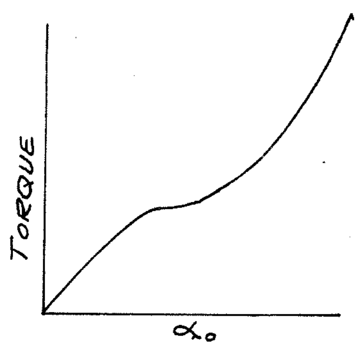

Figure 3a
Assumed non-linearity

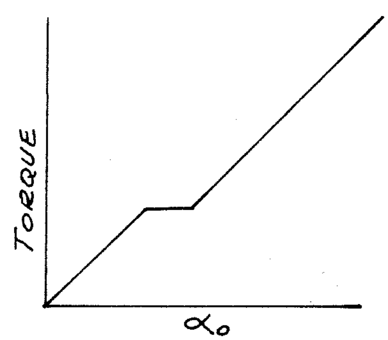

Figure 3b
"flat spot" non-linearity

Such a spring is not commonly encountered in practical structures but it approximates the "flat spot" or "free play" non-linearity which is common to many practical structures. The soft-hard spring has the further advantage of being easily adaptable to the analytical representation of either a purely soft or a purely hard spring. The spring characteristics shown in Figure 3a can be represented by taking the function

$$f_2(\alpha_0) = -\epsilon\alpha_0^3 + \delta\alpha_0^5 \tag{3.47}$$

From equation 3.47 and the definition of $g_2(\alpha_0)$

$$g_2(\alpha_0) = \frac{1}{\pi}\int_0^{2\pi}\left[-\epsilon\alpha_0^2 \sin^4\theta + \delta\alpha_0^4 \sin^6\theta\right] d\theta \tag{3.48}$$

which gives

$$g_2(\alpha_0) = -\frac{3}{4}\epsilon\alpha_0^2 + \frac{5}{8}\delta\alpha_0^4 \tag{3.49}$$

For the specific numerical example chosen the parameters ϵ and δ were taken as

$$\epsilon = 4.00$$

$$\delta = 32.00$$

It should be noted that these values represent small non-linearities provided that

$$\epsilon, \delta \ll \frac{1}{\alpha_0^2}$$

The remaining parameters are those given in section 3.0 for the numerical example treated there.

The results of substituting the numerical values into equation 3.46 are shown plotted in Figure 4. The ordinate for this plot is chosen as $\frac{U^2}{\omega_\alpha^2 b^2}$ or $\frac{1}{k^2 X}$ and the abscissa is $\frac{\omega^2}{\omega_\alpha^2}$ or $\frac{1}{X}$. Thus, Figure 4 is a dimensionless plot of airspeed versus frequency analogous to Figure 2a for the linear case. The effect of the non-linearity is apparent since a different curve is obtained for each value of amplitude, α_0 , as reflected in the term $g_2(\alpha_0)$. The curves can be interpreted as showing that sinusoidal oscillation of the wing is possible at any specified amplitude for all airspeeds below a certain maximum. The occurrence of these maxima suggests a situation similar to that encountered for the aerodynamically conservative linear case, namely that frequency coalescence has occurred and undamped sinusoidal motion is not possible for airspeeds above this maximum. Since the system is non-linear, however, the possibility remains that an increase in airspeed could result in a corresponding change in amplitude and frequency and in the maintainance of undamped sinusoidal motion. Thus the flutter problem for the non-linear case consists of an investigation of the maximum points, or points of frequency coalescence. The problem is better illustrated in Figure 5 where amplitude has been plotted against the airspeed corresponding to frequency coalescence. To make the plot non-dimensional the abscissas have all been divided by the coalescence speed for zero amplitude or, in other words, by the linear flutter speed, U_0 . In the discussion which follows the airspeeds corresponding to frequency coalescence will be referred to as flutter speeds.

The flutter speed and its variation with amplitude can be determined in general form from equation 3.46. For this purpose it is useful to change to variables to

$$u = \frac{U^2}{\omega_\alpha^2 b^2} = \frac{1}{k^2 X} \tag{3.50}$$

$$v = \frac{\omega^2}{\omega_\alpha^2} = \frac{1}{X} \tag{3.51}$$

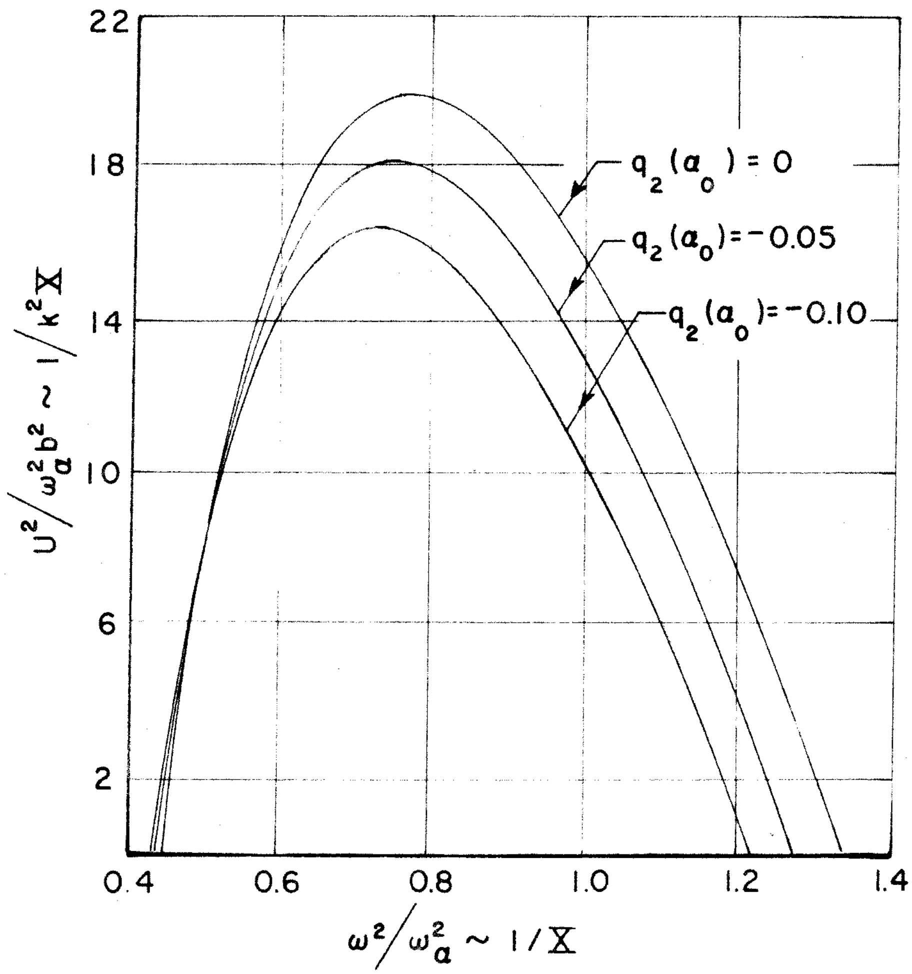

FIG. 4 AIRSPEED-FREQUENCY PLOTS, UNDAMPED CASE

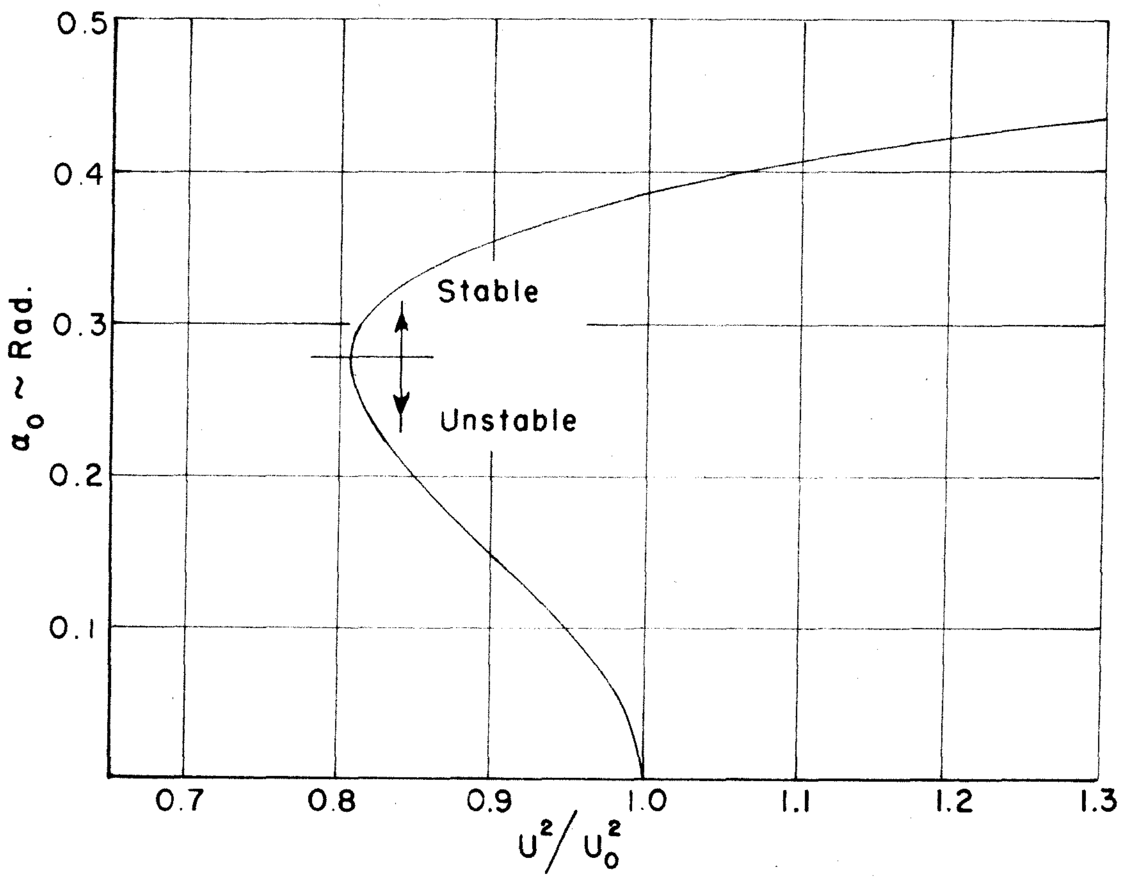

FIG. 5 AMPLITUDE VERSUS AIRSPEED, UNDAMPED CASE

Substitution of these variables into equation 3.46 gives

$$u = \frac{r_\alpha^2 (v - R)\left\{v - X\left[1 + g_2(\alpha_0)\right]\right\}}{\lambda\left[P(v - R) - v x_\alpha\right]} \tag{3.52}$$

The value of v corresponding to flutter is then given by the coalescence condition

$$\frac{du}{dv} = 0 \tag{3.53}$$

This condition then yields

$$v = \frac{1}{P - x_\alpha}\left\{PR - \left[\frac{PR^2 x_\alpha (r_\alpha^2 - P x_\alpha) - R x_\alpha r_\alpha^2 (P - x_\alpha)\left[1 + g_2(\alpha_0)\right]}{\delta^2}\right]^{\frac{1}{2}}\right\} \tag{3.54}$$

Substitution of equation 3.54 into equation 3.52 gives the flutter speed, but the result is too algebraically complicated to be useful. For the purposes at hand, however, it is possible to circumvent this complication by returning to equation 3.45 from which equation 3.46 was derived. Here the flutter condition can be determined by differentiating with respect to v and setting $\frac{du}{dv} = 0$. If equation 3.45 is written

$$f(u, v) = A(G - \mu) - E(C + \mu x_\alpha) = 0$$

then the flutter condition becomes

$$\frac{df}{dv} = \frac{\partial f}{\partial u}\frac{du}{dv} + \frac{\partial f}{\partial v} = 0$$

or, since $\frac{du}{dv} = 0$, this reduces to

$$\frac{\partial f}{\partial v} = 0 \tag{3.55}$$

Equation 3.55 results in

$$A + G - \mu = 0 \tag{3.56}$$

This is the condition for flutter. It should be observed that this is the non-linear counterpart of equation 3.31 which was identified there as the equation for small separation of aeroelastic modal frequencies. The fact that these equations are similar is, of course, not surprising since the system presently being considered can only flutter by a vanishing of the frequency separation due to the absence of aerodynamic damping.

The stability of the flutter motion can now be analyzed by the method of section 2.1. From equations 2.51 through 2.53 and the equations of motion 3.34 through 3.37 the following results are obtained

$$I_1 = -\alpha_0 (C + \mu x_\alpha) \sin\varphi \tag{3.57}$$

$$I_2 = \frac{h_0}{b} E \sin\varphi \tag{3.58}$$

$$I_5 = [A - (G - \mu)] \alpha_0 \frac{h_0}{b} + \left[(C + \mu x_\alpha)\alpha_0^2 - E\frac{h_0^2}{b^2}\right] \cos\varphi \tag{3.59}$$

From which:

$$\frac{\partial I_1}{\partial \frac{h_0}{b}} = 0$$

$$\frac{\partial I_1}{\partial \alpha_0} = -(C+\mu x_\alpha)\sin\varphi - \mu' \alpha_0 x_\alpha \sin\varphi$$

$$\frac{\partial I_1}{\partial \varphi} = -\alpha_0 (C+\mu x_\alpha)$$

$$\frac{\partial I_2}{\partial \frac{h_0}{b}} = E \sin\varphi$$

$$\frac{\partial I_2}{\partial \alpha_0} = 0, \quad \frac{\partial I_2}{\partial \varphi} = E \frac{h_0}{b} \cos\varphi$$

$$\frac{\partial I_5}{\partial \alpha_0} = \frac{h_0}{b}\left[A-(G-\mu)\right] + \mu' \alpha_0 \frac{h_0}{b} + 2\alpha_0 (C+\mu x_\alpha) + \mu' x_\alpha \alpha_0^2$$

$$\frac{\partial I_5}{\partial \frac{h_0}{b}} = \alpha_0\left[A-(G-\mu)\right] - 2E\frac{h_0}{b}$$

$$\frac{\partial I_5}{\partial \varphi} = 0$$

These results can be simplified through the use of the steady state results 3.42 through 3.44 to give

$$\frac{\partial I_1}{\partial \frac{h_0}{b}} = 0$$

$$\frac{\partial I_1}{\partial \alpha_0} = 0$$

$$\frac{\partial I_1}{\partial \varphi} = A\frac{h_0}{b}$$

$$\frac{\partial I_2}{\partial \frac{h_0}{b}} = 0$$

$$\frac{\partial I_2}{\partial \alpha_0} = 0$$

$$\frac{\partial I_2}{\partial \varphi} = -\alpha_0 (G-\mu)$$

$$\frac{\partial I_5}{\partial \frac{h_0}{b}} = (A+G-\mu)\alpha_0$$

$$\frac{\partial I_5}{\partial \alpha_0} = -\frac{h_0}{b}(A+G-\mu) + \mu'\alpha_0\left(\alpha_0 x_\alpha + \frac{h_0}{b}\right)$$

Substituting these into equation 2.60 gives the stability determinantal equation

$$\begin{vmatrix} -2\kappa\beta^2\Omega & 0 & A\frac{h_o}{b} \\ 0 & -2\kappa\beta^2\Omega & -\alpha_o(G-\mu) \\ (A+G-\mu)\alpha_o & -\frac{h_o}{b}(A+G-\mu)+\mu'(\alpha_o x_\alpha+\frac{h_o}{b})\alpha_o & 2\kappa\beta^2\alpha_o\frac{h_o}{b}\Omega \end{vmatrix} = 0 \qquad (3.60)$$

When the determinant in equation 3.60 is expanded the characteristic equation

$$(2\kappa\beta^2\Omega)^2 + (A+G-\mu)^2 - \mu'\alpha_o(G-\mu)\left(\frac{\alpha_o}{\frac{h_o}{b}}x_\alpha + 1\right) = 0 \qquad (3.61)$$

is obtained. This is more conveniently written as

$$2\kappa\beta^2\Omega = \pm\sqrt{-(A+G-\mu)^2 + \mu'(G-\mu)\left(\frac{\alpha_o}{\frac{h_o}{b}}x_\alpha+1\right)\alpha_o} \qquad (3.62)$$

The condition for stability as stated in section 2.1 requires that Ω be a positive number. Since the term $2\kappa\beta^2$ on the left hand side of equation 3.62 is always positive and in view of the $\pm$ sign leading the radical on the right hand side, the condition for stability is simply that the right hand side of equation 3.62 be a pure imaginary, or in other words

$$\mu'\alpha_o(G-\mu)\left(\frac{\alpha_o}{\frac{h_o}{b}}x_\alpha+1\right) < (A+G-\mu)^2 \qquad (3.63)$$

At this point the condition of frequency coalescence, equation 3.56, can be used to advantage. When equation 3.56 is substituted into equation 3.63, the stability condition becomes

$$\alpha_0 \mu' (G-\mu)\left(\frac{\alpha_0}{\frac{h_0}{b}} x_\alpha + 1\right) < 0 \tag{3.64}$$

In the concluding portion of section 2.1 it was observed that the occurrence of a vertical tangent in the plot of amplitude versus flutter speed plays an important role in the determination of system stability. It is thus useful to determine the location of this vertical tangent.

The vertical tangent can be found in general by considering the equations for steady motion, 3.38 through 3.41. If these are written

$$I_1 = \alpha_0 (C + \mu x_\alpha) \sin \varphi = 0 \tag{3.65}$$

$$I_2 = \frac{h_0}{b} E \sin \varphi = 0 \tag{3.66}$$

$$I_3 = \frac{h_0}{b} A + \alpha_0 (C + \mu x_\alpha) \cos \varphi = 0 \tag{3.67}$$

$$I_4 = \frac{h_0}{b} E \cos \varphi + \varphi (G - \mu) = 0 \tag{3.68}$$

it is possible to consider each equation to be in the form

$$I = I\left[\frac{h_0}{b}(\alpha_0), \alpha_0, \varphi(\alpha_0), \kappa^2 \Sigma(\alpha_0), \Sigma(\alpha_0)\right] \tag{3.69}$$

This relationship can be thought of as expressing the fact that equations 3.65 through 3.68 comprise a system of four equations in five unknowns and that the system can be solved for four of the unknowns, $\frac{h_o}{b}$, φ, K^2 and $\mathfrak{X}$ in terms of the fifth unknown α_o. When the system 3.65 through 3.68 is viewed in this manner the vertical tangents are found by taking

$$\frac{dI}{d\alpha_o} = \frac{\partial I}{\partial \frac{h_o}{b}} \frac{d\frac{h_o}{b}}{d\alpha_o} + \frac{\partial I}{\partial \varphi}\frac{d\varphi}{d\alpha_o} + \frac{\partial I}{\partial (K^2\mathfrak{X})}\frac{d(K^2\mathfrak{X})}{d\alpha_o} + \frac{\partial I}{\partial \mathfrak{X}}\frac{d\mathfrak{X}}{d\alpha_o} + \frac{\partial I}{\partial \alpha_o} = 0 \tag{3.70}$$

and setting $\frac{d(K^2\mathfrak{X})}{d\alpha_o}$ and $\frac{d\mathfrak{X}}{d\alpha_o}$ both equal to zero. The resulting equations are:

$$\left[\alpha_o(C+\mu x_\alpha)\cos\varphi\right]\frac{d\varphi}{d\alpha_o} + \left[(C+\mu x_\alpha)\sin\varphi\right] + \alpha_o\mu' x_\alpha \sin\varphi = 0 \tag{3.71}$$

$$A\frac{d\frac{h_o}{b}}{d\alpha_o} - \left[\alpha_o(C+\mu x_\alpha)\sin\varphi\right]\frac{d\varphi}{d\alpha_o} + (C+\mu x_\alpha)\cos\varphi + \alpha_o\mu' x_\alpha\cos\varphi = 0 \tag{3.72}$$

$$\frac{d\frac{h_o}{b}}{d\alpha_o}(E\sin\varphi) + \frac{d\varphi}{d\alpha_o}\frac{h_o}{b}E\cos\varphi = 0 \tag{3.73}$$

$$\frac{d\frac{h_o}{b}}{d\alpha_o}E\cos\varphi - \frac{d\varphi}{d\alpha_o}\frac{h_o}{b}E\sin\varphi + (G-\mu) - \alpha_o\mu' = 0 \tag{3.74}$$

When the steady state results 3.42 through 3.44 are substituted into the above equations, there results from the first three equations:

$$\frac{d\varphi}{d\alpha_o} = 0 \tag{3.75}$$

$$\frac{d\frac{h_o}{b}}{d\alpha_o} = \frac{\frac{h_o}{b}}{\alpha_o} - \frac{\mu' x_\alpha \alpha_o}{A} \tag{3.76}$$

and substituting these together with the steady state results into equation 3.74 gives the condition for a vertical tangent, namely,

$$\alpha_0 \mu' \left[\frac{\alpha_0}{\frac{h_0}{b}} x_\alpha (G-\mu) - A \right] = 0 \tag{3.77}$$

When the condition for frequency coalescence, equation 3.56, is substituted into this result the condition becomes

$$\alpha_0 \mu' (G-\mu) \left(\frac{\alpha_0}{\frac{h_0}{b}} x_\alpha + 1 \right) = 0 \tag{3.78}$$

Comparison of this result with the stability condition 3.64 shows that the stability of the system is completely determined by the pitching amplitude relative to the point of vertical tangency.

The conditions for stable flutter limit cycles and for vertical tangency, equations 3.64 and 3.78, can be greatly simplified through the use of equation 3.56 together with the steady state relations 3.34 through 3.37. Thus

$$\frac{\alpha_0}{\frac{h_0}{b}} = -\frac{E}{G-\mu} = \frac{E}{A} = \frac{R \overline{X} x_\alpha}{p^2 - r_\alpha^2 R \overline{X}}$$

and

$$\alpha_0 \mu' (G-\mu) \left(\frac{\alpha_0}{\frac{h_0}{b}} x_\alpha + 1 \right) = -\alpha_0 \mu' k^2 \overline{X} p^2 (1 - R\overline{X})$$

From the known positive character of the terms α_0, $k^2 \overline{X}$ and p^2 this reduces the stability and vertical tangency conditions to

$$\mu' (1 - R\overline{X}) > 0 \tag{3.79}$$

and

$$\mu'(1-R\Xi) = 0 \tag{3.80}$$

respectively.

For cases of practical interest it can be shown that

$$(1-R\Xi) > 0$$

which reduces equations 3.79 and 3.80 to

$$\mu' > 0 \tag{3.81}$$

$$\mu' = 0 \tag{3.82}$$

From the definition of μ these in turn reduce to

$$g_2'(\alpha_0) > 0 \tag{3.83}$$

$$g_2'(\alpha_0) = 0 \tag{3.84}$$

Equation 3.83 is then both the necessary and the sufficient condition for the existence of stable flutter limit cycles.

For the soft-hard non-linearity given in equation 3.47, equation 3.84 gives for the pitching amplitude corresponding to vertical tangency

$$\alpha_0 = \sqrt{\frac{3\epsilon}{5\delta}} \tag{3.85}$$

and thus for stability

$$\alpha_0 > \sqrt{\frac{3\epsilon}{5\delta}} \tag{3.86}$$

For the numerical example, these relations state that for motion with a pitching amplitude less than $\sqrt{\frac{3\epsilon}{5\delta}}$ or 0.274 radians the system is unstable. This is indicated in Figure 5. Thus the flutter limit cycles corresponding to the lower branch of the curve are unstable, whereas those corresponding to the upper branch are stable.

3.2 The More Exact Non-linear Case

In the preceding section steady state solutions were obtained for the case in which the aerodynamic damping predicted by linear piston theory was neglected. The justification for considering this case lies in the fact that without further assumption it was possible to develop simple stability criteria for the flutter limit cycles. It will be seen in the present section that the aerodynamically damped case presents a more complicated stability problem and that simplification is possible only through recourse to the assumption of small modal frequency separation. For the development of formulas for the limit cycles structural non-linearities will be considered in both the bending and torsional stiffnesses. The equations of motion for this case are given by equations 2.17 and 2.18, and the method of solution is precisely that given in section 2.1. From equations 2.43 through 2.50 the equations of motion reduce to

$$2k\beta^2 \frac{h_0'}{b} = B\frac{h_0}{b} + \left[D\cos\varphi - (C+\mu x_\alpha)\sin\varphi\right]\alpha_0 = I_1 \tag{3.87}$$

$$2k\beta^2 \alpha_0' = \left[(E+\nu x_\alpha)\sin\varphi + F\cos\varphi\right]\frac{h_0}{b} + H\alpha_0 = I_2 \tag{3.88}$$

$$-2k\beta^2 \frac{h_0}{b}\varphi_1' = (A-\nu r_\alpha^2)\frac{h_0}{b} + \left[(C+\mu x_\alpha)\cos\varphi + D\sin\varphi\right]\alpha_0 = I_3 \tag{3.89}$$

$$-2k\beta^2 \alpha_0 \varphi_2' = \left[(E+\nu x_\alpha)\cos\varphi - F\sin\varphi\right]\frac{h_0}{b} + (G-M)\alpha_0 = I_4 \tag{3.90}$$

Where the notation of section 2.1 has been retained. The steady state equations are found as before by setting $\frac{h_o'}{b} = \alpha_o' = \varphi_1' = \varphi_2' = 0$ to give:

$$I_1 = 0 \tag{3.91}$$

$$I_2 = 0 \tag{3.92}$$

$$I_3 = 0 \tag{3.93}$$

$$I_4 = 0 \tag{3.94}$$

Since the algebraic manipulations involved are somewhat intricate, a brief outline will be given of the steps employed in computing the steady state solutions (limit cycles) from equations 3.91 through 3.94. First, equations 3.91 and 3.93 are combined by multiplying equation 3.92 by $\sin\varphi$ and equation 3.91 by $\cos\varphi$ and adding the results to give

$$\left[(A - \nu r_\alpha^2)\sin\varphi + B\cos\varphi\right]\frac{h_o}{b} + D\alpha_o = 0 \tag{3.95}$$

Next, equation 3.93 is multiplied by $\cos\varphi$ and equation 3.91 by $(-\sin\varphi)$ and the results are added to give

$$\left[(A - \nu r_\alpha^2)\cos\varphi - B\sin\varphi\right]\frac{h_o}{b} + (C + \mu x_\alpha)\alpha_o = 0 \tag{3.96}$$

Equations 3.92 and 3.94 are retained in their original forms. The system 3.92, 3.94, 3.95, and 3.96 will now be solved for the limit cycles. Solving equations 3.92 and 3.95 for α_o and equating the results gives

$$\tan\varphi = \frac{BH - DF}{D(E+\nu x_\alpha) - H(A-\nu r_\alpha^2)} \tag{3.97}$$

From equation 3.97

$$\sin\varphi = \frac{BH - DF}{J} \tag{3.98}$$

$$\cos\varphi = \frac{D(E+\nu x_\alpha) - H(A-\nu r_\alpha^2)}{J} \tag{3.99}$$

Where

$$J = \left\{ (BH-DF)^2 + \left[D(E+\nu x_\alpha) - H(A-\nu r_\alpha^2) \right]^2 \right\}^{1/2} \tag{3.100}$$

Substituting equations 3.98 and 3.99 into equation 3.95 gives the amplitude ratio,

$$\frac{\alpha_0}{\frac{h_0}{b}} = \frac{F(A-\nu r_\alpha^2) - B(E+\nu x_\alpha)}{J} \tag{3.101}$$

Next, substituting equations 3.98, 3.99, and 3.101 into equation 3.96 gives

$$(A-\nu r_\alpha^2)\left[D(E+\nu x_\alpha) - H(A-\nu r_\alpha^2)\right] - B(BH-DF) + (C+\mu x_\alpha)\left[A(A-\nu r_\alpha^2) - B(E+\nu x_\alpha)\right] = 0 \tag{3.102}$$

A similar substitution into equation 3.94 gives

$$(E+\nu x_\alpha)\left[D(E+\nu x_\alpha) - H(A-\nu r_\alpha^2)\right] - F(BH-DF) + (G-\mu)\left[F(A-\nu r_\alpha^2) - B(E+\nu x_\alpha)\right] = 0 \tag{3.103}$$

Equations 3.102 and 3.103 can be combined to give the slightly less cumbersome equations

$$\left[F(A-\nu r_\alpha^2)-B(E+\nu x_\alpha)\right]\left[(BH-DF)+(C+\mu x_\alpha)(E+\nu x_\alpha)-(G-\mu)(A-\nu r_\alpha^2)\right]=0 \quad (3.104)$$

$$\left[F(A-\nu r_\alpha^2)-B(E+\nu x_\alpha)\right]\left[D(E+\nu x_\alpha)-H(A-\nu r_\alpha^2)+F(C+\mu x_\alpha)-B(G-\mu)\right]=0 \quad (3.105)$$

It can be shown that flutter does not occur when

$$F(A-\nu r_\alpha^2)-B(E+\nu x_\alpha)=0 \quad (3.106)$$

Therefore, equations 3.104 and 3.105 can be reduced to

$$BH-DF+(C+\mu x_\alpha)(E+\nu x_\alpha)-(G-\mu)(A-\nu r_\alpha^2)=0 \quad (3.107)$$

$$D(E+\nu x_\alpha)-H(A-\nu r_\alpha^2)+F(C+\mu x_\alpha)-B(G-\mu)=0 \quad (3.108)$$

The occurrence of the functions $\mu(\alpha_0)$ and $\nu\left(\frac{h_0}{b}\right)$ in equations 3.107 and 3.108 shows the explicit dependence of the limit cycles on the amplitudes. In principle, the actual limit cycles can be determined by eliminating dependence on one of the amplitudes through equation 3.101. For the purposes at hand, however, it will be sufficient to solve equations 3.107 and 3.108 for the flutter speed parameter $K^2 X$ and for the frequency ratio X in terms of the general non-linear functions $g_1\left(\frac{h_0}{b}\right)$ and $g_2(\alpha_0)$. This can be done by removing the compressed notation from the equations. When this is done equation 3.107 gives

$$K^2 \bar{X} = \frac{\omega_\alpha^2 b^2}{U^2} = \frac{\lambda \bar{X}\left\{P\left[1 - R\bar{X}(1+g_1)\right] - x_\alpha\right\} + \lambda^2 (Q - P^2)\bar{X}}{r_\alpha^2\left[1 - \bar{X}(1+g_2)\right]\left[1 - R\bar{X}(1+g_1)\right] - x_\alpha^2} \qquad (3.109)$$

Equation 3.77 gives

$$\bar{X} = \frac{\omega_\alpha^2}{\omega^2} = \frac{-2Px_\alpha + Q + r_\alpha^2}{RQ(1+g_1) + r_\alpha^2(1+g_2)} \qquad (3.110)$$

Equations 3.109 and 3.110 compare directly with equations 3.6 and 3.7 for the linear case. The amplitude dependence is apparent through the appearance of the functions $g_1\left(\frac{h_0}{b}\right)$ and $g_2(\alpha_0)$, and it is seen that setting $g_1 = g_2 = 0$ gives the results for the linear case.

When the non-linearity is limited to the torsional stiffness, equations 3.109 and 3.110 can be plotted in a manner identical with that shown for the undamped case of Figure 5. Such a plot is shown in Figure 6 for the same set of parameters and assumed non-linearity as was used for the undamped example. It can be seen that the behavior is the same with the flutter speed being reduced for the smaller values of amplitude and increased for the larger ones. A plot such as this completely defines the system limit cycles and the only problem remaining is an investigation of the stability of these limit cycles.

The procedure for determining the limit cycle stability is given in section 2.1 and will be followed here. Again, for simplicity, the non-linearity will be confined to the torsional stiffness.

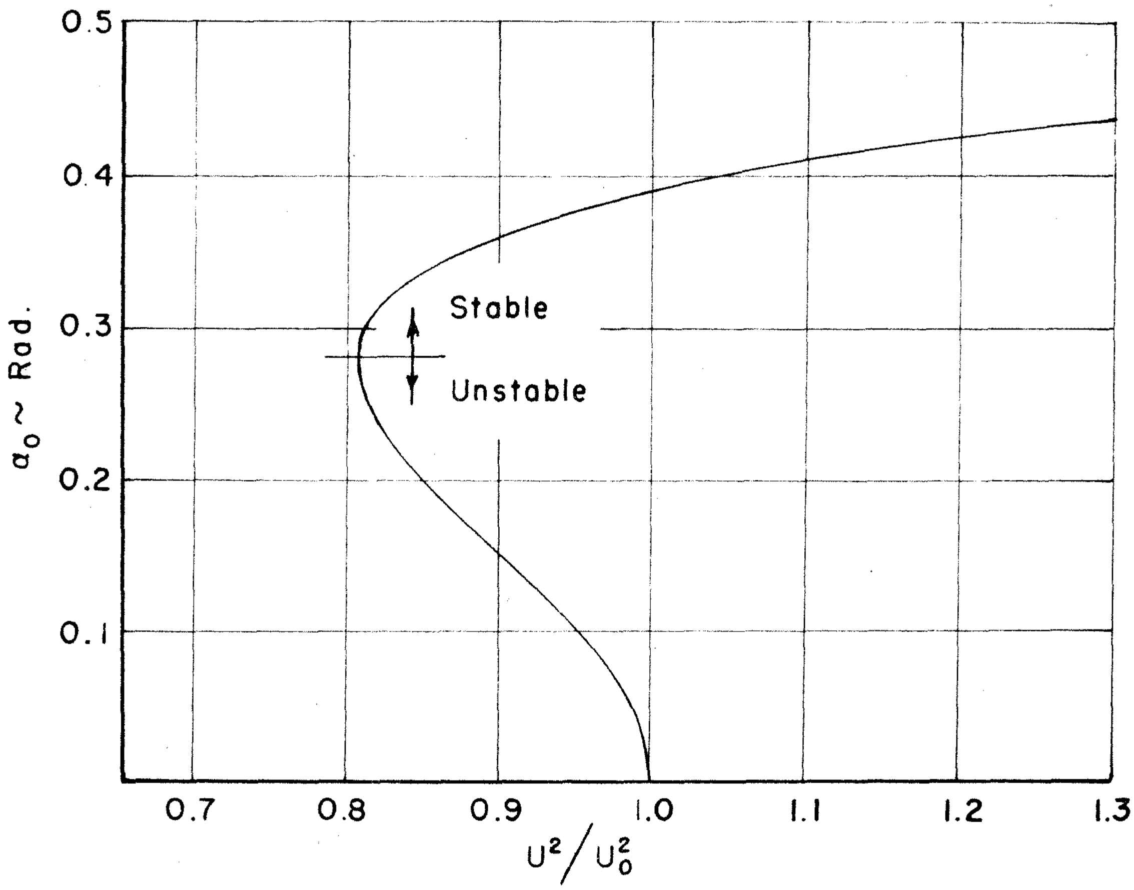

FIG. 6 AMPLITUDE VERSUS AIRSPEED WITH AERODYNAMIC DAMPING

From equations 3.87 through 3.90 and the assumption of steady state behavior

$$I_1 = B\frac{h_o}{b} + [D\cos\varphi - (C+\mu x_\alpha)\sin\varphi]\alpha_o = 0 \tag{3.111}$$

$$I_2 = [E\sin\varphi + F\cos\varphi]\frac{h_o}{b} + H\alpha_o = 0 \tag{3.112}$$

$$I_5 = [A-(G-\mu)]\alpha_o\frac{h_o}{b} + [(C+\mu x_\alpha)\cos\varphi + D\sin\varphi]\alpha_o^2 - [E\cos\varphi - F\sin\varphi]\frac{h_o^2}{b^2} = 0 \tag{3.113}$$

From which:

$$\frac{\partial I_1}{\partial \frac{h_o}{b}} = B$$

$$\frac{\partial I_1}{\partial \alpha_o} = [-(C+\mu x_\alpha)\sin\varphi + D\cos\varphi] - \alpha_o\mu' x_\alpha \sin\varphi$$

$$\frac{\partial I_1}{\partial \varphi} = \alpha_o[-(C+\mu x_\alpha)\cos\varphi - D\sin\varphi]$$

$$\frac{\partial I_2}{\partial \frac{h_o}{b}} = E\sin\varphi + F\cos\varphi$$

$$\frac{\partial I_2}{\partial \alpha_o} = H$$

$$\frac{\partial I_2}{\partial \varphi} = \frac{h_o}{b}[E\cos\varphi - F\sin\varphi]$$

$$\frac{\partial I_5}{\partial \frac{h_o}{b}} = [A-(G-\mu)]\alpha_o - 2[E\cos\varphi - F\sin\varphi]\frac{h_o}{b}$$

$$\frac{\partial I_5}{\partial \alpha_o} = [A-(G-\mu)]\frac{h_o}{b} + \alpha_o\frac{h_o}{b}\mu' + 2\alpha_o[(C+\mu x_\alpha)\cos\varphi + D\sin\varphi] + \alpha_o^2\mu' x_\alpha\cos\varphi$$

$$\frac{\partial I_5}{\partial \varphi} = \alpha_o^2[-(C+\mu x_\alpha)\sin\varphi + D\cos\varphi] + \frac{h_o^2}{b^2}[E\sin\varphi + F\cos\varphi]$$

These expressions can be simplified through the use of the steady state relations 3.91 through 3.94 to give:

$$\frac{\partial I_1}{\partial \alpha_0} = -\frac{B\frac{h_0}{b}}{\alpha_0} - \alpha_0 \mu' x_2 \sin\varphi \quad , \quad \frac{\partial I_1}{\partial \varphi} = A\frac{h_0}{b}$$

$$\frac{\partial I_2}{\partial \frac{h_0}{b}} = -H\frac{\alpha_0}{\frac{h_0}{b}} \quad , \quad \frac{\partial I_2}{\partial \varphi} = -(G-\mu)\alpha_0$$

$$\frac{\partial I_5}{\partial \frac{h_0}{b}} = (A+G-\mu)\alpha_0 \, , \quad \frac{\partial I_5}{\partial \alpha_0} = -(A+G-\mu)\frac{h_0}{b} + \alpha_0\frac{h_0}{b}\mu'\left(1+\frac{\alpha_0}{\frac{h_0}{b}}x_\alpha \cos\varphi\right)$$

$$\frac{\partial I_5}{\partial \varphi} = -\alpha_0\frac{h_0}{b}(B+H)$$

When the above expressions are substituted into the stability determinant 2.60 there results

$$\begin{vmatrix} B-2\kappa p^2\Omega & -\left(\frac{B\frac{h_0}{b}}{\alpha_0} + \alpha_0\mu' x_2 \sin\varphi\right) & A\frac{h_0}{b} \\ -H\frac{\alpha_0}{\frac{h_0}{b}} & H-2\kappa p^2\Omega & -(G-\mu)\alpha_0 \\ (A+G-\mu)\alpha_0 & -(A+G-\mu)\frac{h_0}{b} + \alpha_0\frac{h_0}{b}\mu'\left(1+\frac{\alpha_0}{\frac{h_0}{b}}x_\alpha\cos\varphi\right) & -\alpha_0\frac{h_0}{b}\left[(B+H)+2\kappa p^2\Omega\right] \end{vmatrix} = 0$$

(3.114)

Expansion of this determinant gives the characteristic polynomial

$$
\begin{aligned}
&(2k\beta^2\Omega)^3 - 2(B+H)(2k\beta^2\Omega)^2 + (2k\beta^2\Omega)\Big[(B+H)^2 + (A+G-\mu)^2 \\
&- \mu'(G-\mu)\alpha_0\Big(1+\frac{\alpha_0}{\frac{h_0}{b}}x_\alpha\cos\varphi\Big) - \mu' x_\alpha H\frac{\alpha_0^2}{\frac{h_0}{b}}\sin\varphi\Big] + \mu'\alpha_0\Big\{\big[B(G-\mu)-AH\big] \\
&\Big(1+\frac{\alpha_0}{\frac{h_0}{b}}x_\alpha\cos\varphi\Big) + \frac{\alpha_0}{\frac{h_0}{b}}x_\alpha\sin\varphi\big[H(B+H) \\
&+ (A+G-\mu)(G-\mu)\big]\Big\} = 0
\end{aligned}
\tag{3.115}
$$

The stability of the limit cycles can now be determined by application of the Routh-Hurwitz criteria as given in equations 2.62 through 2.66. Before doing this, however, it will be useful to examine the relative magnitudes of the terms in equation 3.115.

It was stated in section 3.0 that consideration would be limited to systems for which the aerodynamic damping is small and thus systems for which the modal frequency separation is small. This assumption was shown to lead to equation 3.31

$$A + G = O(\epsilon) \tag{3.31}$$

Consequently, since the function $\mu(\alpha_0)$ is of order ϵ , we can write

$$(A+G-\mu) = O(\epsilon) \tag{3.116}$$

Similarly, the condition of small damping expressed as

$$\lambda^2(Q-P^2) = O(\epsilon) \tag{3.117}$$

together with equations 3.98 and 3.101 and the definition of the term H leads to the result that

$$H \frac{\alpha_o}{\frac{h_o}{b}} \sin\varphi = O(\epsilon) \tag{3.118}$$

Finally, the term $\mu'(\alpha_o)$ is of order ϵ by definition. Thus, when terms of order higher than ϵ are dropped from equation 3.115, the following cubic polynomial is obtained:

$$(2k\rho^2\Omega)^3 - 2(B+H)(2k\rho^2\Omega)^2 + 2k\rho^2\Omega\Big[(B+H)^2 - \mu'(G-\mu)\alpha_o\Big(1+\frac{\alpha_o}{\frac{h_o}{b}}x_\alpha\cos\varphi\Big)\Big] + \mu'\alpha_o\Big\{(B+H)(G-\mu)\Big(1+\frac{\alpha_o}{\frac{h_o}{b}}x_\alpha\cos\varphi\Big)\Big\} = 0 \tag{3.119}$$

The Routh-Hurwitz criteria, when applied to equation 3.119 give the following inequalities which must be satisfied for stability:

$$-2(B+H) > 0 \tag{3.120}$$

$$(B+H)^2 - \mu'(G-\mu)\alpha_o\Big(1+\frac{\alpha_o}{\frac{h_o}{b}}x_\alpha\cos\varphi\Big) > 0 \tag{3.121}$$

$$\mu'\alpha_o(B+H)(G-\mu)\Big(1+\frac{\alpha_o}{\frac{h_o}{b}}x_\alpha\cos\varphi\Big) > 0 \tag{3.122}$$

$$-2(B+H)\Big[(B+H)^2 - \mu'(G-\mu)\alpha_o\Big(1+\frac{\alpha_o}{\frac{h_o}{b}}x_\alpha\cos\varphi\Big)\Big] > (B+H)(G-\mu)\mu'\alpha_o\Big(1+\frac{\alpha_o}{\frac{h_o}{b}}x_\alpha\cos\varphi\Big) \tag{3.123}$$

The inequality 3.120 is seen to be satisfied immediately from the definitions of B and H which give

$$B + H = \lambda K \left[2 P x_\alpha - Q - r_\alpha^2 \right] \tag{3.124}$$

Equation 3.110 applied to the present case becomes

$$X = \frac{\omega_\alpha^2}{\overline{\omega}^2} = \frac{-2Px_\alpha + Q + r_\alpha^2}{RQ + r_\alpha^2(1+g_z)} \tag{3.125}$$

Since X must be greater than zero for flutter to exist and since the denominator of equation 3.94 is always positive for small non-linearities it is seen that

$$-2Px_\alpha + Q + r_\alpha^2 > 0 \tag{3.126}$$

Inequality 3.95 together with equation 3.93 and the known positive character of the parameters λ and K gives

$$B + H < 0 \tag{3.127}$$

which demonstrates the validity of inequality 3.120. Having established the validity of inequality 3.120, a small amount of algebraic manipulation of inequalities 3.121 through 3.123 shows that each is satisfied provided that

$$\mu' \alpha_0 (G - \mu)\left(1 + \frac{\alpha_0}{\frac{h_0}{b}} x_\alpha\right) < 0 \tag{3.128}$$

Comparison of this result with inequality 3.64 shows that the stability criteria for both the passive and aerodynamically damped systems are identical through the first power in ϵ .

In sections 2.1 and 3.1 it was shown that the criterion for stability could be identified with the relationship between the flutter amplitude and the amplitude for which a vertical tangent occurs on a plot of amplitude versus flutter speed. It will now be shown that this is true for the present case.

As in the case of the passive aerodynamic system the vertical tangent is found from the steady state equations. If these are written

$$I_1 = B\frac{h_0}{b} + \left[-(C+\mu x_\alpha)\sin\varphi + D\cos\varphi\right]\alpha_0 = 0 \qquad (3.129)$$

$$I_2 = \left[E\sin\varphi + F\cos\varphi\right]\frac{h_0}{b} + H\alpha_0 = 0 \qquad (3.130)$$

$$I_3 = A\frac{h_0}{b} + \left[(C+\mu x_\alpha)\cos\varphi + D\sin\varphi\right]\alpha_0 = 0 \qquad (3.131)$$

$$I_4 = \left[E\cos\varphi - F\sin\varphi\right]\frac{h_0}{b} + (G-\mu)\alpha_0 = 0 \qquad (3.132)$$

the system can be considered as a set of four equations in the five unknowns $\alpha_0, \frac{h_0}{b}, \varphi, K^2\bar{X}$ and $\bar{X}$. Noting that at a vertical tangent

$$\frac{d(K^2\bar{X})}{d\alpha_0} = \frac{d\bar{X}}{d\alpha_0} = 0 \qquad (3.133)$$

the following result is obtained from equations 3.98 and 3.99

$$\frac{dI_1}{d\alpha_0} = \frac{\partial I_1}{\partial \frac{h_0}{b}}\frac{d\frac{h_0}{b}}{d\alpha_0} + \frac{\partial I_1}{\partial\varphi}\frac{d\varphi}{d\alpha_0} + \frac{\partial I_1}{\partial\alpha_0} = 0 \qquad (3.134)$$

$$\frac{dI_2}{d\alpha_0} = \frac{\partial I_2}{\partial \frac{h_0}{b}} \frac{d\frac{h_0}{b}}{d\alpha_0} + \frac{\partial I_2}{\partial \varphi} \frac{d\varphi}{d\alpha_0} + \frac{\partial I_2}{\partial \alpha_0} = 0 \tag{3.135}$$

Thus, at the vertical tangent

$$\frac{d\frac{h_0}{b}}{d\alpha_0} = - \frac{\begin{vmatrix} \frac{\partial I_1}{\partial \alpha_0} & \frac{\partial I_1}{\partial \varphi} \\ \frac{\partial I_2}{\partial \alpha_0} & \frac{\partial I_2}{\partial \varphi} \end{vmatrix}}{\begin{vmatrix} \frac{\partial I_1}{\partial \frac{h_0}{b}} & \frac{\partial I_1}{\partial \varphi} \\ \frac{\partial I_2}{\partial \frac{h_0}{b}} & \frac{\partial I_2}{\partial \varphi} \end{vmatrix}} = \frac{\left[B(G-\mu)-AH\right]\frac{h_0}{b} + \mu'(G-\mu)\alpha_0^2 x_\alpha \sin\varphi}{\alpha_0\left[B(G-\mu)-AH\right]} \tag{3.136}$$

$$\frac{d\varphi}{d\alpha_0} = - \frac{\begin{vmatrix} \frac{\partial I_1}{\partial \frac{h_0}{b}} & \frac{\partial I_1}{\partial \alpha_0} \\ \frac{\partial I_2}{\partial \frac{h_0}{b}} & \frac{\partial I_2}{\partial \alpha_0} \end{vmatrix}}{\begin{vmatrix} \frac{\partial I_1}{\partial \frac{h_0}{b}} & \frac{\partial I_1}{\partial \alpha_0} \\ \frac{\partial I_2}{\partial \frac{h_0}{b}} & \frac{\partial I_2}{\partial \alpha_0} \end{vmatrix}} = \frac{-\alpha_0^2}{\frac{h_0}{b}} H \mu' x_\alpha \sin\varphi \tag{3.137}$$

From equations 3.131 and 3.132

$$\frac{dI_3}{d\alpha_0} = \frac{\partial I_3}{\partial \frac{h_0}{b}} \frac{d\frac{h_0}{b}}{d\alpha_0} + \frac{\partial I_3}{\partial \varphi} \frac{d\varphi}{d\alpha_0} + \frac{\partial I_3}{\partial \alpha_0} = 0 \tag{3.138}$$

$$\frac{dI_4}{d\alpha_0} = \frac{\partial I_4}{\partial \frac{h_0}{b}} \frac{d\frac{h_0}{b}}{d\alpha_0} + \frac{\partial I_4}{\partial \varphi} \frac{d\varphi}{d\alpha_0} + \frac{\partial I_4}{\partial \alpha_0} = 0 \tag{3.139}$$

These equations, upon substitution of equations 3.136 and 3.137 then give

$$\mu'\left\{\frac{\alpha_o^2}{\frac{h_o}{b}} x_\alpha \sin\varphi\left[A(G-\mu)+BH\right] + \frac{\alpha_o^2}{\frac{h_o}{b}} x_\alpha \cos\varphi\left[B(G-\mu)-AH\right]\right\}=0 \tag{3.140}$$

and

$$\mu'\left\{x_\alpha \frac{\alpha_o^2}{\frac{h_o}{b}}\left[(G-\mu)^2+H^2\right]\sin\varphi + \alpha_o\left[B(G-\mu)-AH\right]\right\} = 0 \tag{3.141}$$

Equations 3.140 and 3.141 are the conditions for the occurrence of a vertical tangent. When the two equations are added the result is

$$\begin{aligned}\alpha_o\mu'\Big\{&\Big(1+\frac{\alpha_o}{\frac{h_o}{b}} x_\alpha\cos\varphi\Big)\left[B(G-\mu)-AH\right] + \frac{\alpha_o}{\frac{h_o}{b}} x_\alpha \sin\varphi\Big[(G-\mu)(A+G-\mu)\\ &+H(B+H)\Big]\Big\} = 0\end{aligned} \tag{3.142}$$

Comparison of this result with the last term of the stability equation 3.115 shows that the vanishing of the constant term and thus a sufficient condition for the occurrence of neutral stability is the occurrence of a vertical tangent in the amplitude-velocity curve. Following the order of magnitude arguments of the preceding paragraphs it can be shown that up to terms of the order of ϵ^2 equation 3.111 reduces to

$$\alpha_o\mu'(G-\mu)\Big(1+\frac{\alpha_o}{\frac{h_o}{b}} x_\alpha\Big) = 0 \tag{3.143}$$

which is identical with the vertical tangent condition for the undamped case as given in equation 3.78. When the condition of small frequency separation,

$$A + G - \mu = O(\epsilon) \tag{3.144}$$

is employed, together with the steady state equations 3.129 through 3.132, equations 3.128 and 3.144 can be reduced to

$$g_2' > 0 \tag{3.145}$$

$$g_2' = 0 \tag{3.146}$$

These relations, in turn, show that for the soft-hard spring characteristic chosen in the numerical example the system is unstable for amplitudes less than the amplitude at which the vertical tangent occurs.

CHAPTER IV

NUMERICAL RESULTS AND LIMIT CYCLE STABILITY

Since the results of the preceding sections are somewhat obscured by algebraic complication it is felt that several numerical examples will be useful both for purposes of illustration and for quantitative evaluation of the assumptions pertinent to the analysis. In the discussion which follows three numerical examples of steady state limit cycles are given. For one of these examples, the one chosen for subsequent analysis on the analog computer, the limit cycle stability is investigated numerically and from the relative sizes of the stability roots and the system parameters an *a posteriori* check is made on the "slowly varying" assumption.

4.1 Steady State Solutions

The three examples chosen for numerical evaluation were variations of the example given in Chapter Three. A single parameter of this system, the elastic axis location x_o, was varied from mid chord to the airfoil quarter chord. Since the elastic axis location is reflected only in the parameters P and Q these are the only parameters which change for the cases investigated*. A summary of these parameters is given below.

*For an airfoil of fixed geometric and inertia properties a variation in the parameter x_o results in a variation of the other dimensionless parameters of the system as well. For this reason the three cases given here represent airfoils with significantly different physical characteristics.

Case	x_o	P	Q
I	0.50	0	0.33333
II	0.40	0.20	0.37333
III	0.25	0.50	0.58333

All remaining parameters are given in Chapter Three. From equations 3.97, 3.101, 3.109, and 3.110 numerical solutions for the variation of amplitude reduced frequency and phase angle with airspeed were obtained for Cases I and II. The results are given in Figures 7 and 8. The general features exhibited by the two cases are the same. The most striking of these features is the double valued nature of the amplitude curves. Both the pitching and plunging amplitudes exhibit this characteristic for airspeeds below the linear flutter speed. It should be noted that the upper branch of the α_o curve should be read in conjunction with the upper branch of the $\frac{h_o}{b}$ curve and similarly the two lower branches should be read together. In contrast with the amplitudes, however, the reduced frequency and phase angle are each represented by a single valued curve. At first glance this would appear to indicate the absence of amplitude dependence from these two features of the flutter solution. Examination of the defining equations 3.98 and 3.101, however reveals that when non-linearity is absent from the bending stiffness ($\nu = 0$) the reduced frequency and the phase angle are completely determined by the amplitude ratio $\frac{\alpha_o}{h_o/b}$ and the airspeed. Thus the single valued character of these curves implies

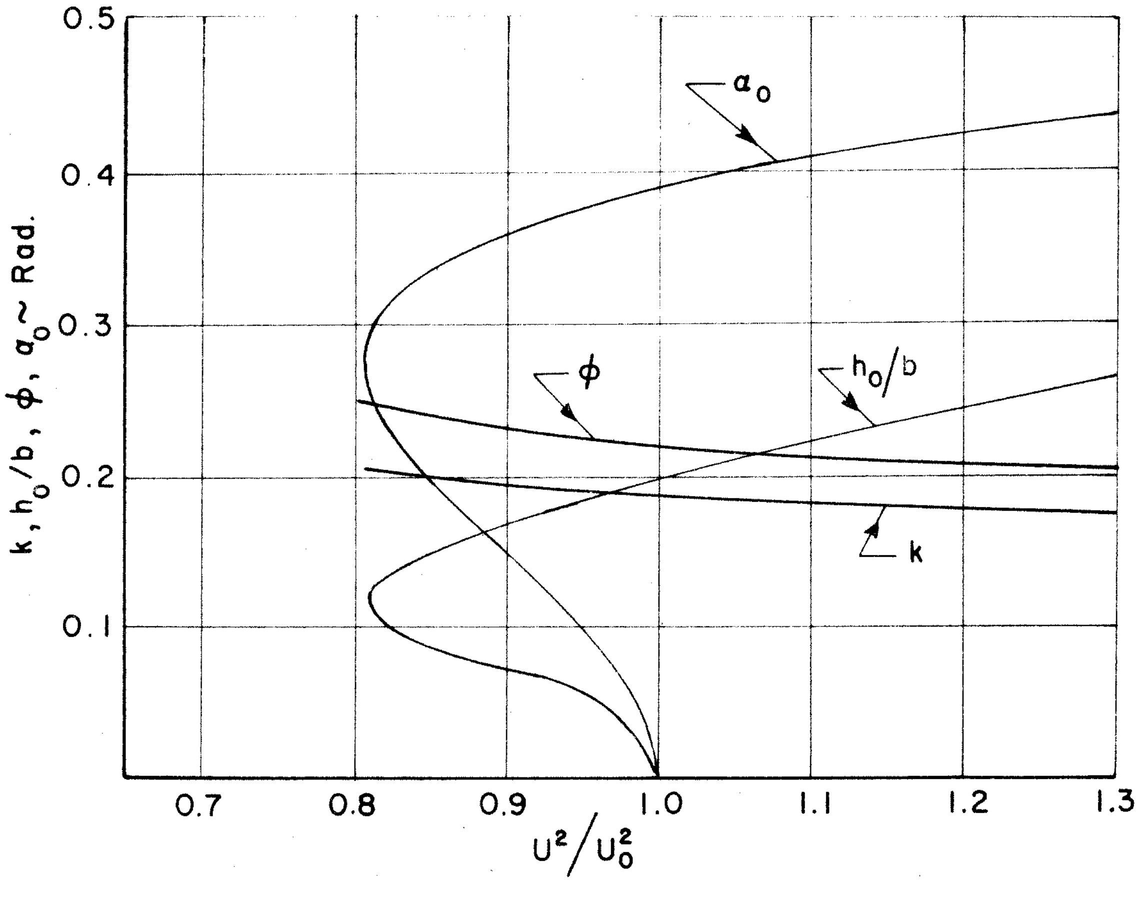

FIG. 7 LIMIT CYCLE SOLUTIONS, CASE I, $X_0 = 0.50$

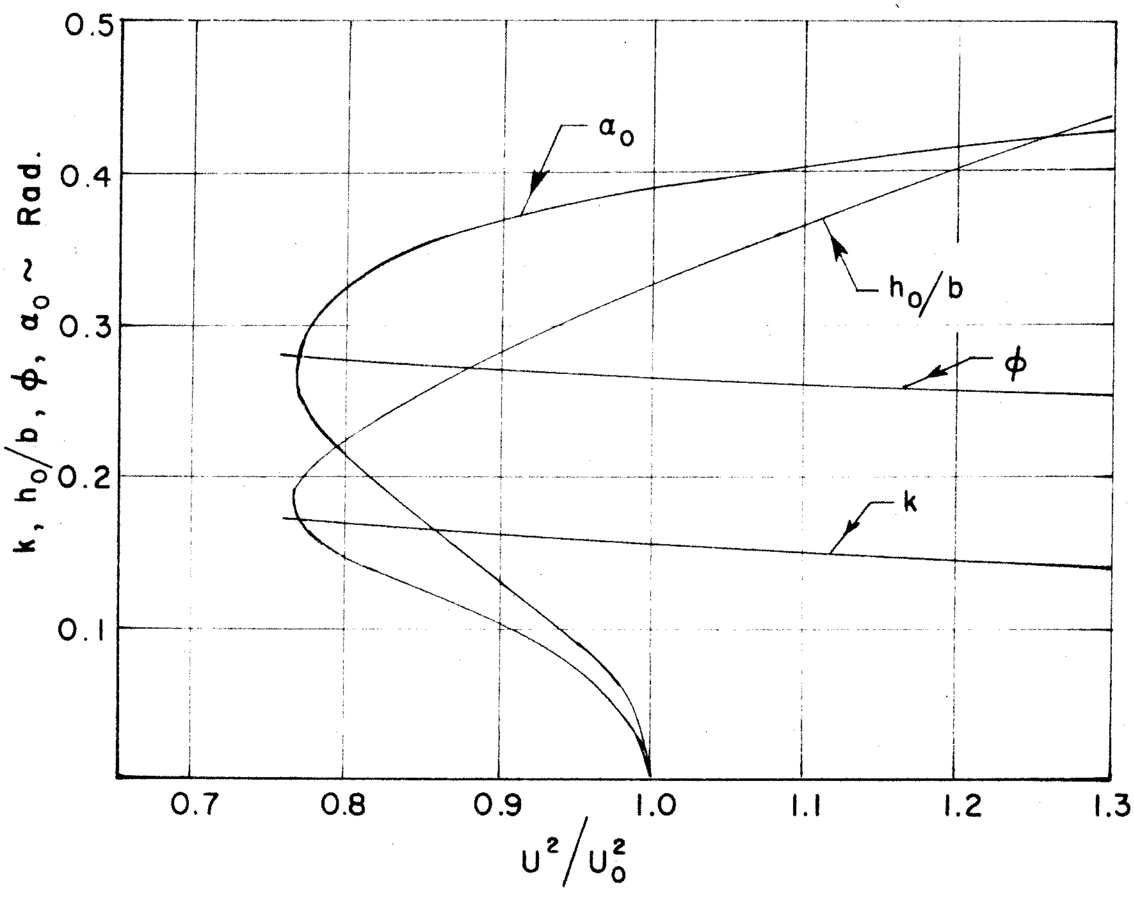

FIG. 8 LIMIT CYCLE SOLUTIONS, CASE 2, $X_0 = 0.40$

that for a given airspeed the amplitude ratio must be identical in each of the two possible limit cycles.

Case III represents a situation peculiar to non-linear systems. When the airfoil parameters for this case are substituted into equations 3.6 and 3.7 to determine the linear flutter speed it is found that no such speed exists. Thus linear theory predicts that this system will be flutter free for all possible airspeeds. When the corresponding equations for non-linear flutter, equations 3.109 and 3.110, are employed a different situation is seen to hold true. A brief discussion of this phenomenon will be given below.

Non-linear flutter of a linearly flutter free system is not surprising when the non-linearity contains a spring softening characteristic. The torsion spring used for the present numerical example was of the "soft-hard" type sketched in Figure 9a.

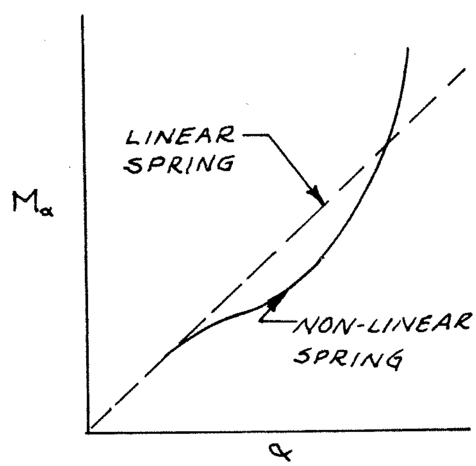

Figure 9a

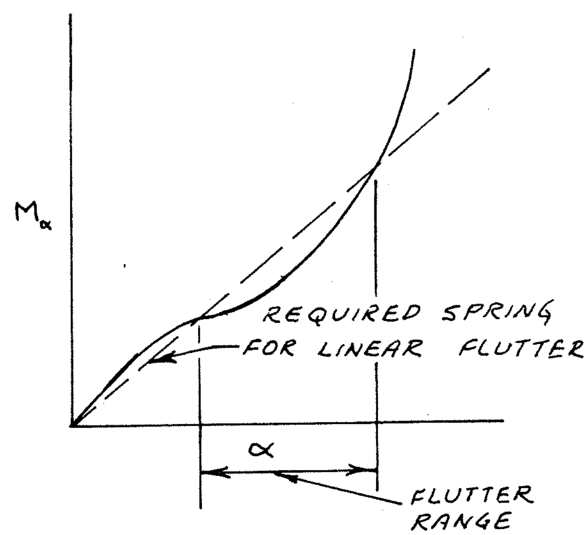

Figure 9b

If the system requires a reduced spring rate to exhibit flutter as illustrated in Figure 9b the soft-hard spring has the potential of providing this if the softening characteristic is sufficiently pronounced. When this happens the airfoil exhibits a range of torsional amplitudes for which flutter is possible.

Case III fulfills the requirements for this type of behavior and the flutter limit cycles are given as functions of airspeed in Figure 10. The asymptotic values of torsional amplitude were obtained by setting K^2 equal to zero in equations 3.109 and 3.110 and solving for α_o. The abscissa of Figure 10 was not normalized by the linear flutter speed since for this case the linear flutter speed was infinite.

4.2 Stability of the Steady State Solutions

The steady state solutions given in the preceding section were each analyzed for stability with respect to small disturbances. For this purpose equation 3.115 was used. In Chapter Three this equation was greatly simplified through the use of the assumptions of small non-linearity and small frequency separation. On the basis of this simplified equation it was shown that the necessary and sufficient condition for limit cycle stability with a soft-hard spring characteristic was that the amplitude of oscillation be greater than the amplitude corresponding to the occurrence of a vertical tangent on the amplitude-airspeed plot. The assumption of small non-linearity is not well satisfied by the torsional spring characteristic chosen for this study and consequently the more complicated equation 3.115 was used for the stability study. This equation is a cubic polynomial in the perturbation

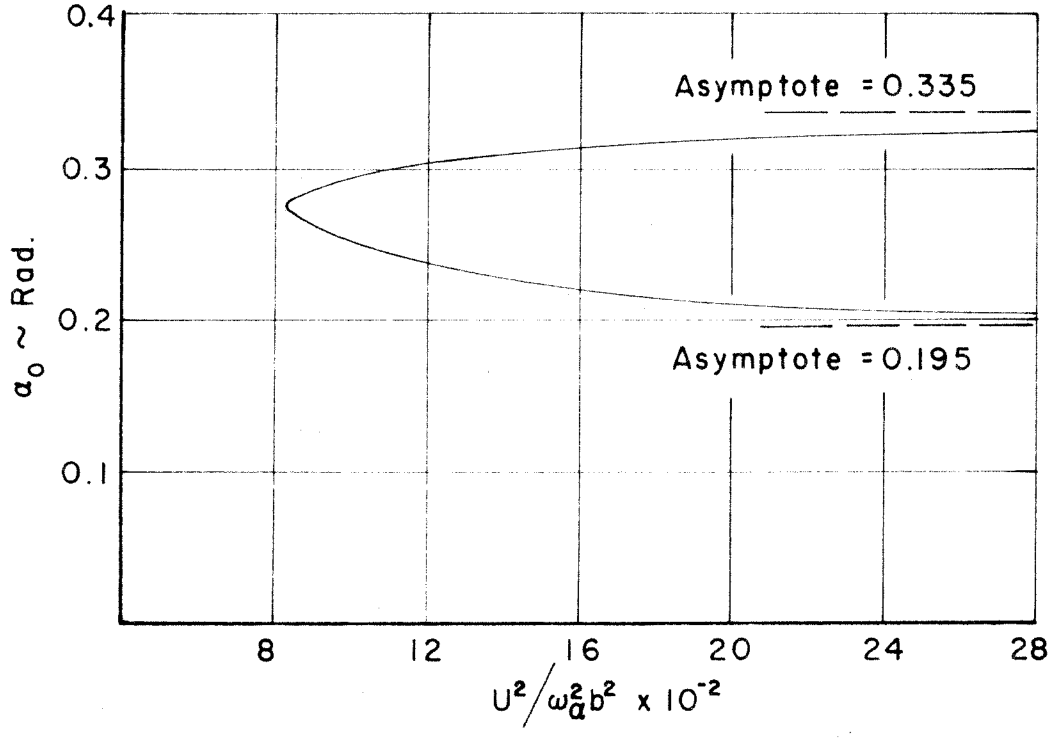

FIG. 10 NON-LINEAR FLUTTER OF A LINEARLY STABLE SYSTEM, CASE 3, $x_0 = 0.25$

exponent Ω and as such is extremely cumbersome with respect to the determination of roots. For this reason only the Routh-Hurwitz criteria were used for stability study of Cases I and III while a single case, Case II was analyzed by determination of the roots of the stability equation throughout the range of torsional amplitude, α_0.

Application of the Routh-Hurwitz criteria to each of the cases investigated showed that the conclusions of Chapter Three were valid, namely, the limit cycles are stable provided their amplitudes exceed the amplitude for vertical tangency. The stability ranges are indicated in Figures 8, 9, and 10.

The roots of equation 3.115 as applied to Case II are shown plotted versus pitching amplitude in Figure 11. It was found that for all values of pitching amplitude the roots to the equation consisted of a single real root and a pair of conjugate complex roots symbolized by:

$$\Omega = \begin{cases} \Omega_1 \\ [\Omega_2]_R + i[\Omega_{2I}] \\ [\Omega_3]_R + i[\Omega_{3I}] \end{cases}$$

Quantitative determination of the roots of the stability equation provides an <u>a posteriori</u> check on the assumption of slowly varying response. It should be noted that the <u>a posteriori</u> viewpoint is a necessary one since at no point in the analysis was the condition of slowly varying response imposed on the system. Rather, it was assumed that the response possessed this character.

From Figure 11 it can be seen that for the range of α_0 below 0.274, the point of vertical tangency, the real root of the stability equation is always positive. For values of α_0 above this point all

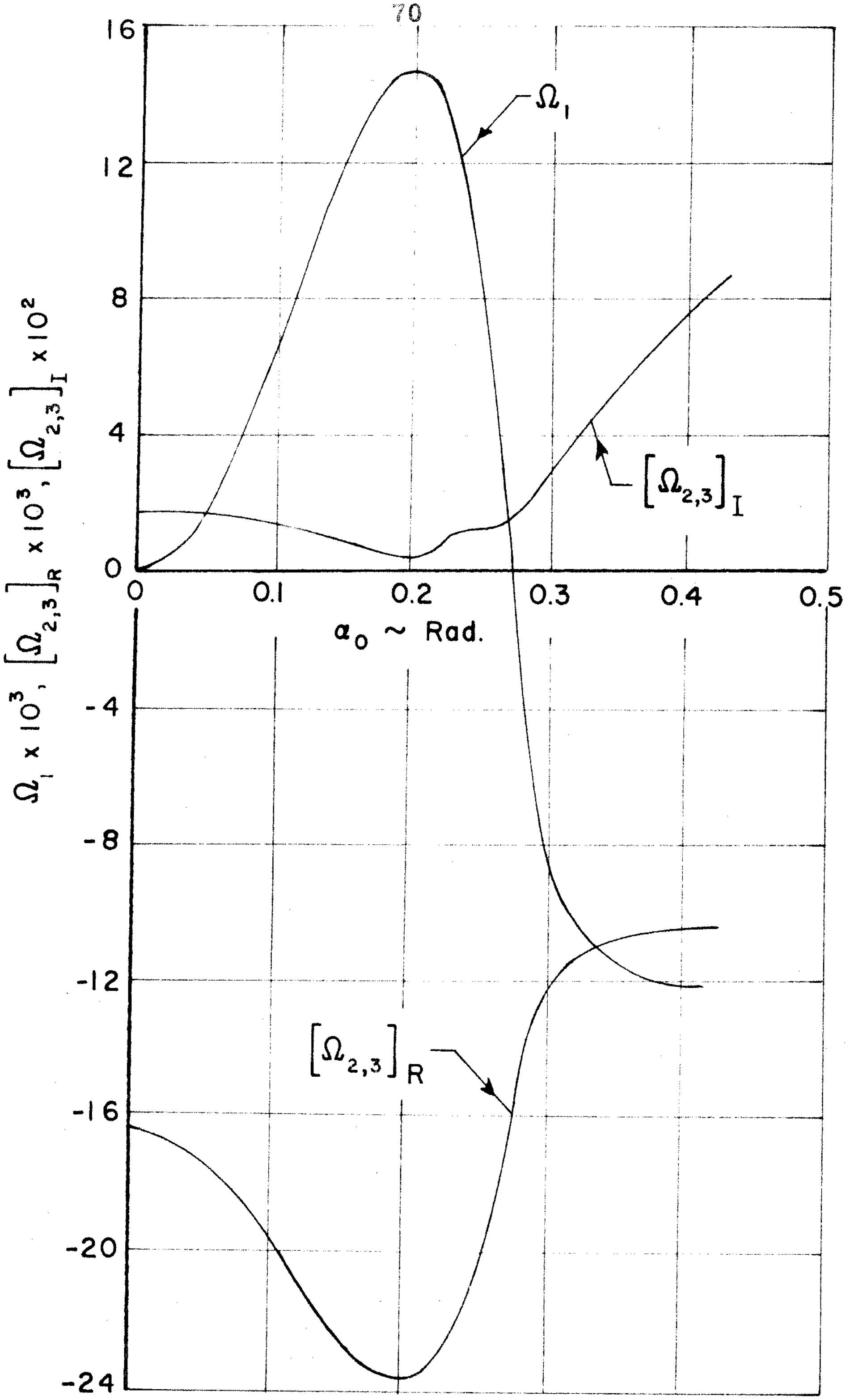

FIG. 11 STABILITY ROOTS, CASE 2, $x_0 = 0.40$

real roots are negative thus substantiating the conclusion of the preceding chapter that the steady state solutions are unstable below the vertical tangency and stable above.

The magnitudes of the roots will be examined for two amplitude values. The first will be an amplitude of 0.20 which corresponds with a value of $\frac{U^2}{U_o^2}$ of 0.815. This point was chosen since it corresponds to the largest real roots for the unstable solutions. The second amplitude to be investigated will be 0.365 which corresponds to a value of $\frac{U^2}{U_o^2}$ of 0.905 and a case investigated with the analog computer and reported in the next chapter. These cases are summarized in the table below where the values of the roots together with the values of reduced frequency are given.

α_o	$\frac{U^2}{U_o^2}$	Ω_1	$[\Omega_{2,3}]_R$	$[\Omega_{2,3}]_I$	K
0.200	0.815	0.0148	-0.0238	0.004	0.167
0.365	0.905	-0.0118	-0.0106	0.061	0.162

The nature of the roots for the first case shows that the response consists of a divergence together with a damped oscillatory motion. An index to the rate of variation of the response is the time required for the perturbation to diverge (or converge) to twice (or one-half) of its initial value. The significant unit of this time is periods of the unperturbed steady state oscillation. The number, η, of these periods is given by

$$\eta = \frac{.693\,K}{2\pi\Omega}$$

For the first case:

$$\eta = 1.24 \quad \text{(divergence)}$$

$$\eta = 0.62 \quad \text{(oscillatory subsidence)}$$

For the second case:

$$\eta = 1.52 \quad \text{(subsidence)}$$

$$\eta = 1.68 \quad \text{(oscillatory subsidence)}$$

Considering only the divergent or subsident motions these numbers can be interpreted as showing that the perturbation amplitude in the first case reaches 161 °/o of its initial value in one cycle and in the second case is diminished to 33 °/o of its initial value in one cycle. These are not what can be considered slow variations. It should be noted, however, that when the perturbations are small with respect to the steady state amplitude (say 10 °/o) the total variation of amplitude per cycle (6 °/o) and 3 °/o respectively for these cases) is within the admissable range. A further check will be obtained from the analog solution reported in the next chapter and several conclusions concerning the general usefulness of the method will be given in Chapter Six of this report.

CHAPTER V

ANALOG COMPUTER SOLUTIONS AND INITIAL CONDITION DEPENDENCE

In the preceding analytical work it was necessary to limit consideration to steady state solutions and their stability. This was due to the mathematical difficulty associated with the solution of equations 2.47 through 2.50. To obtain an idea of the nature of the flutter dependence on initial conditions, therefore, it was decided to obtain an exact numerical solution to the equations of motion for a particular set of airfoil parameters. Initial conditions were provided in the analog solution by starting the airfoil motion with an initial angle of attack.

5.1 The Analog Set Up

Solutions were obtained using the analog computer of the Douglas Aircraft Company, El Segundo Division. This computer is of the differential analyzer type and had more than adequate amplifier capacity for the solution of the present problem. The polynomial nonlinearity was generated using a combination of Douglas Quadratron squaring elements and a multiplier. A schematic diagram of the analog set up is given in Figure 12. The equations of motion are given there with the correct coefficients for the case chosen to be solved here, namely, Case II of the preceding chapter. The dependent variables shown in the figure are related to the variables of the preceding chapters by

$$x_1 = \frac{h}{b}$$

$$x_2 = \alpha$$

$$\ddot{x}_1 = -0.2\ddot{x}_2 - 0.0173(\dot{x}_1 + x_2) - 0.025\,\beta^2 x_1 - 0.0318\,\dot{x}_2$$

$$\ddot{x}_2 = -0.8x_1 - 0.0169\,\ddot{x}_2 - 0.05\,\beta^2\,(x_2 - 4x_2^3 + 32\,x_2^5) - 0.01019\,\dot{x}_1 - 0.01019\,x_2$$

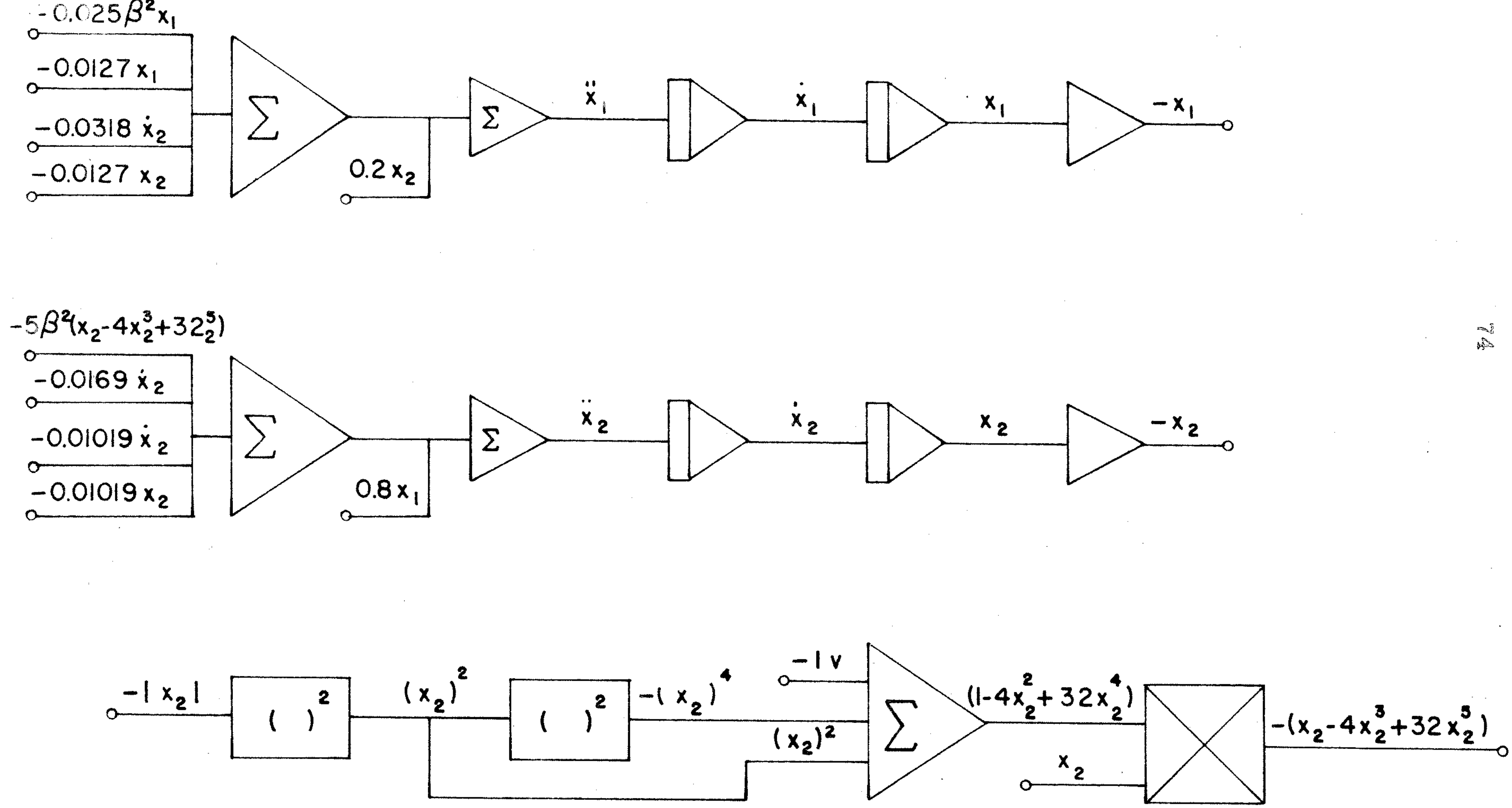

FIG. 12 SCHEMATIC DIAGRAM OF ANALOG ARRANGEMENT

The airspeed, U is determined by the parameter β which is given by

$$\beta^2 = .614 \frac{U_o^2}{U^2}$$

Initial conditions were imposed on the x_2 circuit by the conventional scheme of impressing a prescribed voltage across the capacitor of the x_2 integrator prior to beginning a solution.

5.2 The Analog Solutions

The general character of the analog solutions was as follows:

1. For a range of airspeeds below the linear flutter speed a critical value of initial angle of attack was found to exist. When the airfoil motion was initiated from angles of attack above this critical value, the airfoil was observed to execute oscillations which diverged until reaching a steady state limiting value. When motion was initiated from angles of attack below the critical value the airfoil executed damped oscillations and ultimately returned to rest.

2. A critical airspeed, less than the linear flutter speed, was found such that the airfoil was completely stable for all airspeeds less than this value. In the present sense completely stable indicates that no value of initial angle of attack could be found which resulted in steady airfoil oscillations, instead for every initial angle the airfoil executed damped oscillations and ultimately returned to rest.

3. For airspeeds above the linear flutter speed the rest position of the airfoil was found to be unstable, i.e. any finite initial angle of attack caused the airfoil to execute divergent oscillations until reaching a limiting value.

4. For each airspeed (greater than the critical value mentioned in 2 above) it was found that the amplitude of steady oscillations had a specific value characteristic of that airspeed.

5. Initial angles of attack which exceeded the steady state limiting value were found to result in oscillations which decreased in amplitude until reaching the steady state limit. Therefore steady oscillations were maintained.

The results of the analog investigations of Case II of Chapter Four are given in Figures 13 through 16. Figure 13 shows the most significant of the analog results. Here angle of attack or torsional amplitude is plotted versus the airspeed ratio U^2/U_o^2 in analogy with the plots of the preceding chapters. Shown on the same figure is a plot of the theoretical limit cycle amplitude-airspeed relationship previously obtained. The analog data are plotted in such a manner that both the locus of critical initial conditions and the steady state limiting amplitudes are shown on one double valued but continuous curve. It can be seen from the figure that the agreement between the analog and theoretical stable limit cycles is quite good for the entire airspeed range. More interesting, however, is the fact that the locus

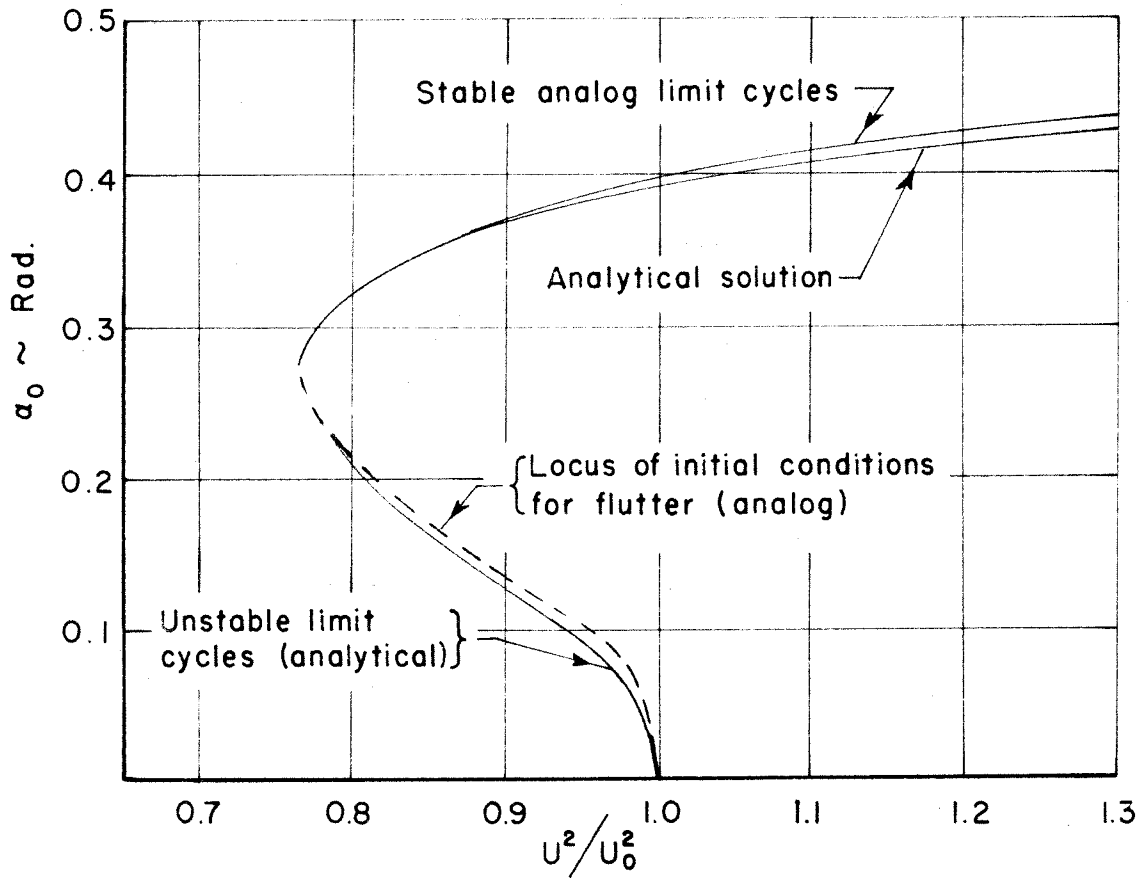

FIG. 13 COMPARISON OF ANALYTICAL AND ANALOG SOLUTIONS

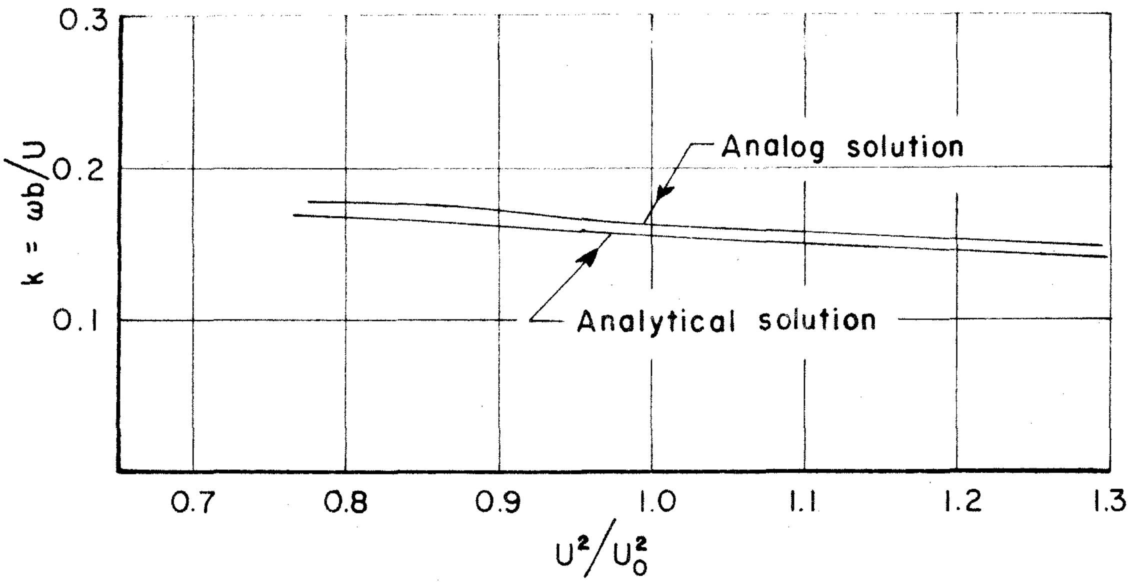

FIG. 14 COMPARISON OF ANALYTICAL AND ANALOG SOLUTIONS

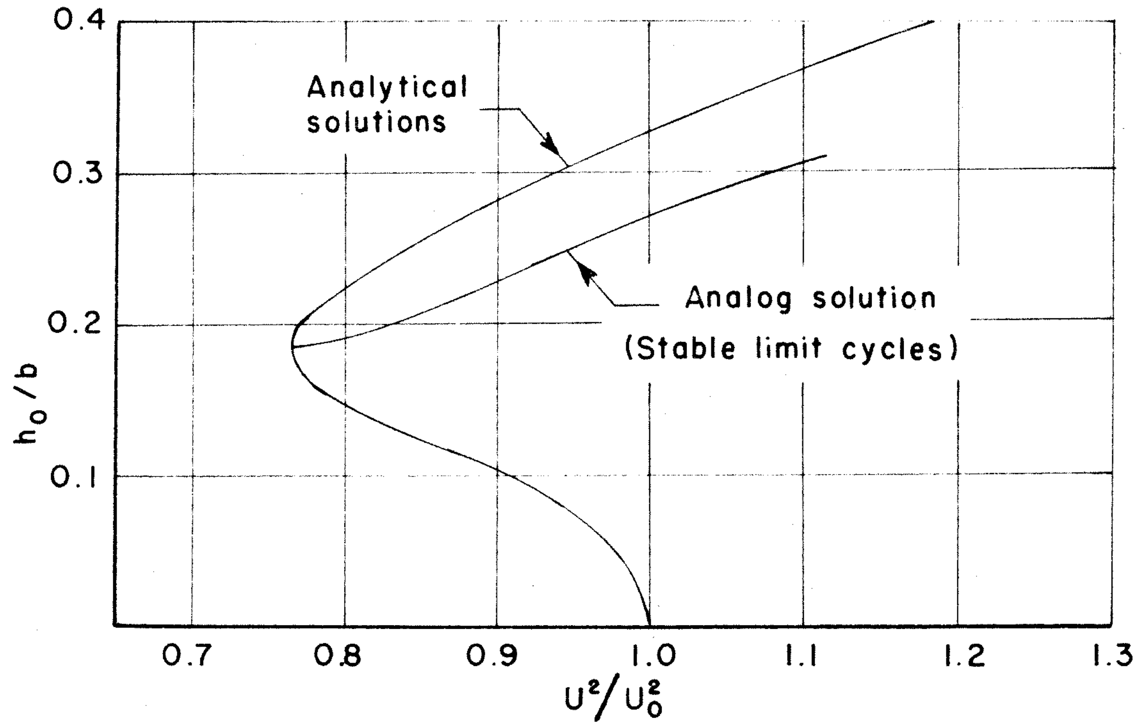

FIG. 15 COMPARISON OF ANALYTICAL AND ANALOG SOLUTIONS

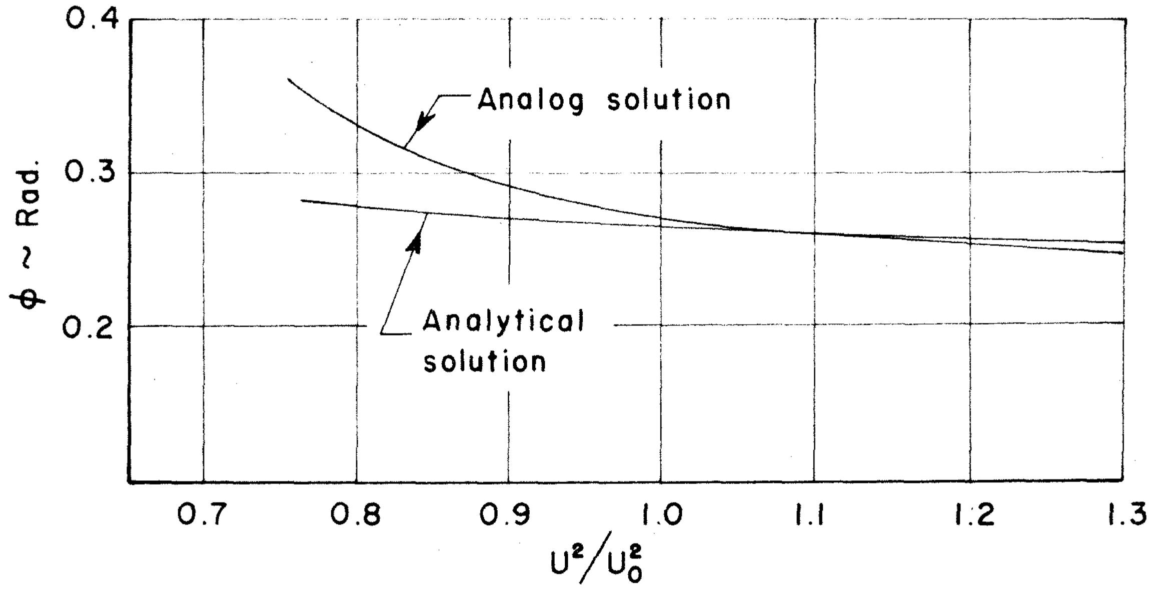

FIG. 16 COMPARISON OF ANALYTICAL AND ANALOG SOLUTIONS

of initial values necessary to cause flutter coincides quite well with the amplitude-airspeed plot of the unstable theoretical limit cycles. Thus it would appear that while the theoretical treatment was limited to steady state behavior, a good estimate was obtained of the initial condition dependence of the flutter system. Figure 14 shows the agreement obtained between the analog and theoretical values of reduced frequency. Here the analog frequency referred to is the reduced frequency of the steady state oscillations or limit cycles. It can be seen that the agreement is good. Figure 16 shows a comparison of the steady state bending amplitudes, $\frac{h_0}{b}$, as obtained theoretically and by the analog computer. The agreement shown is not as good as for the torsional amplitude. The error increases from about 8 ^{o}/o at the lowest flutter speed to nearly 20 ^{o}/o in the intermediate speed range. Figure 16 shows the steady state phase angle between the torsional and bending displacements, the analog and theoretical values compared. Here again some error is apparent.

Some typical time histories of displacement versus dimensionless time ($\tau = \frac{Ut}{b}$) are given in Figures 17 and 18. Figure 17 shows three plots of displacement versus time for a value of U^2/U_0^2 of 0.915. The three initial conditions, α_i , were chosen as shown in the sketch below

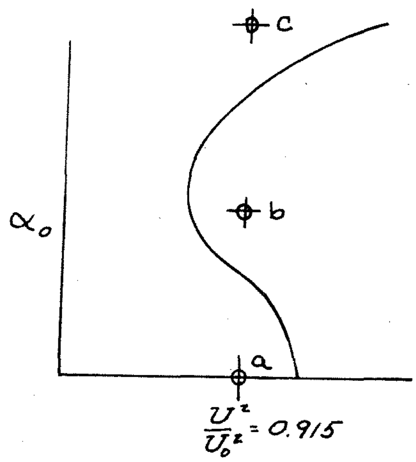

Figure 17a shows the stability of the rest position. Figure 17b shows the response to an initial displacement of 0.20 radians. This initial displacement lies above the amplitude of the unstable limit cycle for this airspeed and consequently diverges to the stable value. It is interesting to note that the maximum change in amplitude per cycle is 36 $^{o}/o$. Figure 17c shows the torsional reponse to an initial displacement of 0.39 radians. Here it is observed that the maximum change in amplitude per cycle never exceeds 10 $^{o}/o$. Thus it appears that when initial values lie in the neighborhood of the stable limit cycle the assumption of slow variation of amplitude is reasonably well satisfied. Although no supporting time history data are presented here, it was also found that a similar situation holds true for initial values which lie in the neighborhood of the unstable limit cycle. In this case it was found that a large number of cycles are executed near the initial value before the system diverges to the stable amplitude. It was concluded from this that the success of the analytical method in the prediction of

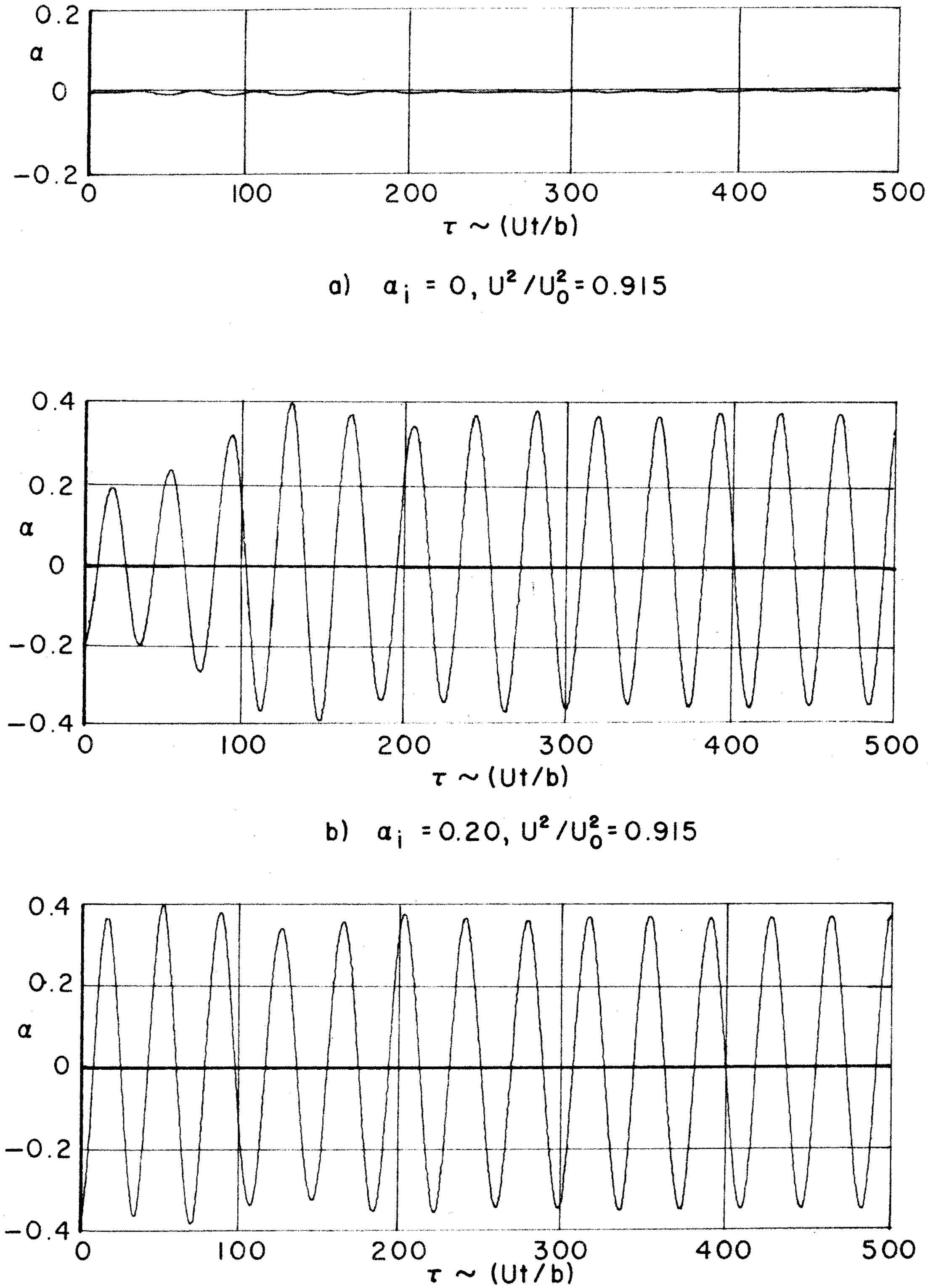

a) $\alpha_i = 0, U^2/U_0^2 = 0.915$

b) $\alpha_i = 0.20, U^2/U_0^2 = 0.915$

c) $\alpha_i = 0.39, U^2/U_0^2 = 0.915$

FIG. 17 ANALOG TIME HISTORIES

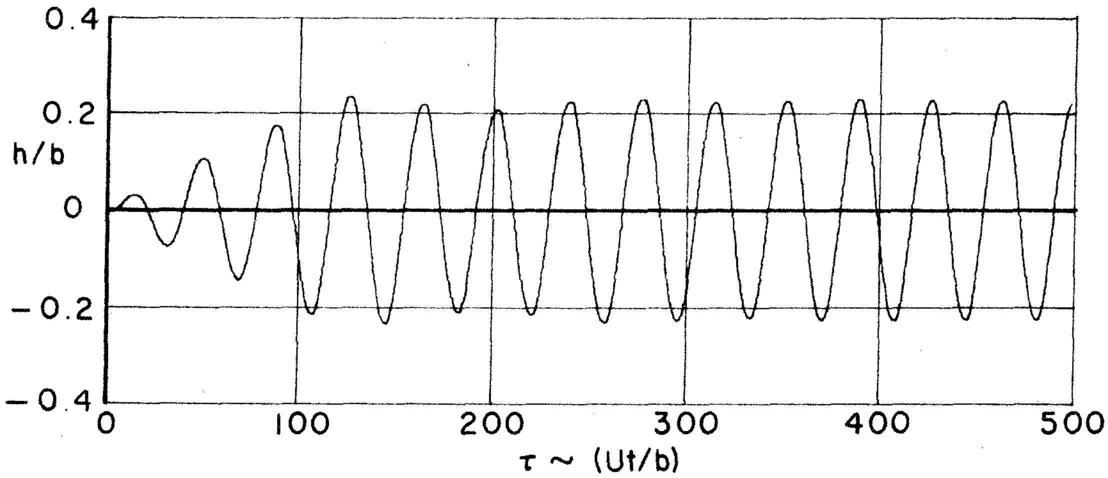

a) $\alpha_i = 0.20, U^2/U_0^2 = 0.915$

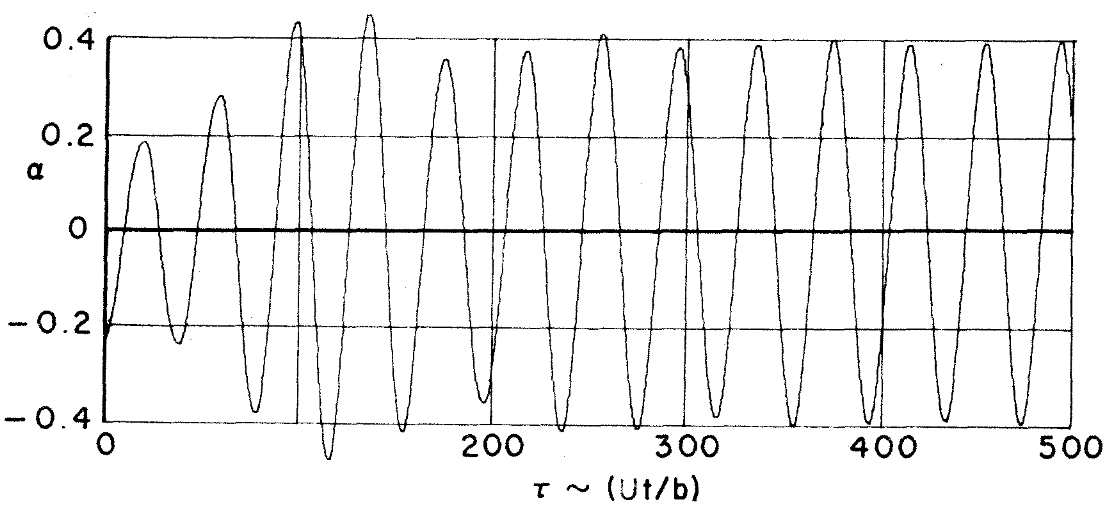

b) $\alpha_i = 0.22, U^2/U_0^2 = 1.06$

FIG. 18 ANALOG TIME HISTORIES

torsional limit cycle amplitudes was due to the validity of the fundamental assumption of slowly varying torsional amplitude near the limit cycle itself. Figure 18a shows the bending response of the system for the case corresponding with Figure 17b. Figure 18b shows the torsional response for an airspeed beyond the linear flutter speed, namely $\frac{U^2}{U_o^2} = 1.06$. The initial displacement was 0.22 radians which placed the system in the rapidly varying category. It can be seen that for any airspeed ratio, initial conditions which are far removed from any limit cycle, either stable or unstable, result in rapidly varying behavior. For this reason it was concluded that the analytical method is not well suited to the prediction of arbitrary initial condition dependence unless the system chosen for investigation is fortuitously slowly varying for the complete amplitude range. Thus equations 2.47 through 2.50 are suitable only for the prediction of limit cycles and their stability.

Figure 19 represents a plot of torsional velocity versus torsional amplitude. The plot is thus a two-dimensional projection of the four-dimensional phase space whose coordinates are α, $\dot{\alpha}$, $\frac{h}{b}$ and $\frac{\dot{h}}{b}$. The figure represents a plot of $\dot{\alpha}$ versus α while $\frac{h}{b}$ and $\frac{\dot{h}}{b}$ take on their full range of values. The limit cycle is apparent from the heavy concentration of trajectories traced out as the system gradually achieved steady state behavior. A feature which distinguishes this phase projection from the familiar one degree of freedom phase space is the fact that the amplitude during the transient motion can exceed the steady state limit. This fact is attributed to the influence of the motion in the other degree of freedom.

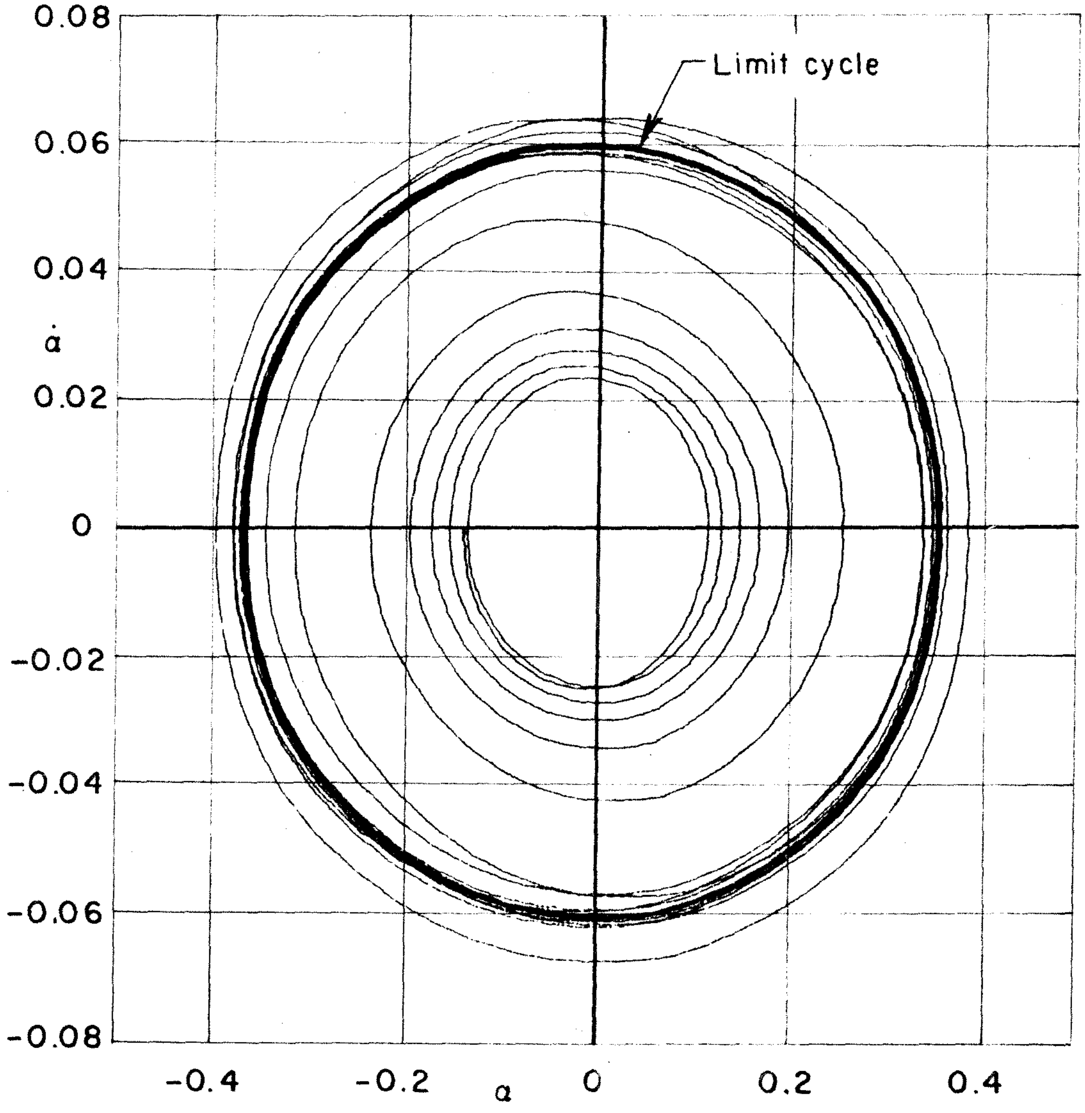

$\alpha_i = 0.14$; $U^2/U_0^2 = 0.915$

FIG. 19 PHASE PLOT OF ANALOG SOLUTION

CHAPTER VI

CONCLUSIONS

The analysis of the preceding chapters was aimed at the evaluation of certain effects of structural non-linearity in a particular flutter problem. The broad range of phenomena associated with flutter in general and the mathematical complication typical of non-linear problems makes the drawing of completely general conclusions very difficult. For this reason the conclusions given below are of a somewhat qualitative nature.

It was found in chapters four and five by an a posteriori approach that the assumption of slowly varying response is not valid for all possible problems of the type considered. This fact is sufficient to lead to the conclusion that a general analysis of the transient flutter problem by the Kryloff and Bogoliuboff method is not possible. It was shown, however, that transient response to initial conditions which place the system near a limit cycle, lead to slowly varying response and under this restriction the method appears to be applicable. This is true, as well, of the situation in which a limit cycle is given a small perturbation and stability is analyzed by observing the transient behavior of the perturbation.

An additional qualification to the applicability of the method is necessary before the stability analysis given here can be justified. Since the assumed form for the steady state solution consisted of only the first harmonic it is necessary that the system considered possess a response in which this term predominates. An example of a system for which this assumption is not justified is given in Reference 4. The analog computer solutions given in the present report, however, show that the response is well represented by the first harmonic term.

In summary, the following list of conclusions is given:

(1) The Kryloff and Bogoliuboff method or method of slowly varying parameters provides a useful technique for the approximate solution of flutter problems in which structural non-linearity plays a role. This is especially true when the aerodynamic forces can be represented in a quasi-steady manner as was done here via piston theory.

(2) For the case of bending-torsion flutter with a non-linear torsion spring of the "soft-hard" type the limit cycle solutions are unstable at amplitudes below the one corresponding to a vertical tangent on a plot of amplitude versus airspeed. This conclusion is subject to the restriction that the frequency separation of the aero-elastic modes is small at the flutter speed.

(3) The amplitude of the unstable limit cycles obtained by the approximate analysis method of the present study were found to provide a good estimate of the initial displacement required to initiate flutter.

(4) The numerical examples investigated in this study revealed that the transient behavior of the flutter system is not, in general, slowly varying. For this reason it is concluded that the Kryloff and Bogoliuboff assumption is not well suited to the determination of transient behavior.

It is, however, suitable for the approximate determination of steady state solutions and their stability since in this case both the assumption of slowly varying response and the assumption that the response is well approximated by the first harmonic term are satisfied.

REFERENCES

1. Fung, Y. C., The Theory of Aeroelasticity, John Wiley and Sons, New York, 1955.

2. Kryloff, N. and Bogoliuboff, N., Introduction to Non-Linear Mechanics, Princeton University Press, 1947.

3. Caughey, T. K., The Existence and Stability of Periodic Motion in Forced, Non-Linear Oscillation, Ph.D. Thesis, California Institute of Technology, 1954.

4. Fung, Y. C., On Two-Dimensional Panel Flutter, Journal of the Aeronautical Sciences, Volume 25, Number 3, March 1958.